**Manuscript revision (doi:10.5194/bg-2016-212): Responses to the Associate Editors comments:**

We thank Jack Middelburg for his helpful and constructive comments that we have taken into account for our manuscript.


L. 14 and all through: use "pore-water" with hyphen if an adjective

We added a hyphen.

L. 15: reformulate TA is not a concentration

Indeed, TA is the equivalent of the weak bases in seawater.
We reformulated:
TA and concentrations of DIC, $SO_4^{2-}$ and $Ca^{2+}$ were analyzed on bottom waters and extracted sediment pore waters, whereas pH and oxygen concentrations were measured *in situ* using microelectrodes.

L. 19: delete aerobic: you cannot see the difference between re-oxidation and aerobic respiration from OPD.

We deleted the word aerobic.

L. 22: aerobic processes, oxic conditions: hence use aerobic here

The word oxic was replaced by the word aerobic.

L. 74: I do not understand this. The knowledge presented in Berners' 1980 book is sufficient to explain all this. Reformulate.

We reformulated the sentence:
 These authors, with Froelich et al. (1979) and Berner (1980) as precursors,  highlighted the complexity of the multiple competing reaction pathways in anoxic sediment.

L. 101: delete differs

We deleted the word differs.

L. 140: sediment accumulation or sediment deposition?

In contrast to the systems like the Amazonas delta, the sediment in the prodelta of the Rhône is not caracterized by intense reworking and fluidized beds, but characterized by high deposition rates that lead to high accumulation rates. We reformulated:
The seafloor in this region is a dynamic environment based on sediment deposition and accumulation and with important heterogeneity regarding diagenetic activities, sediment pore water profiles and exchange fluxes at the sediment-water interface (Lansard et al., 2009; Cathalot et al., 2010).

L. 283/284: TA is not a concentration: rewrite

We reformulated into : DIC concentrations and TA

L. 299: Existing numerical tools have been developed…. Water column. Nevertheless we used…….
Is the neglect of metabolites in TA calculation not the real problem?

We rephrased:
Existing numerical tools have been developed for the oxic water column. Nevertheless we used them in the sediments knowing that pore water concentrations (e.g. DIC, TA) are much larger than those in the water column and that reduced metabolites are neglected.

L. 313: indicate high sulfate..

We added a subordinate:
The distal domain is characterized by constant $Ca^{2+}$ concentrations which remain above 10 mmol $L^{-1}$ and the sulfate concentrations stay close to bottom water concentration.

L. 334-352: this whole section needs referencing. These reaction have been worked out in detail by Boudreau, Soetaert and others.

References were added to the whole paragraph.

L. 360: denitrification pathway does not involved re-oxidation because N2 escapes and thus contributes disproportionally.

We added:
Denitrification forms an exception to this, as the reduced end products $N_2$ of this reaction can escape the sediments. Thus the TA produced by denitrification is not consumed in the oxic sediment layer.

L. 372: I suggest deleting aerobic. Not needed and geochemists have since appreciated more re-oxidation.

We deleted the word aerobic.

L. 435: Denitrification section should mention that N2 is not oxidized and thus TA can escape.

We added:
Nevertheless denitrification is a net TA source from the sediments to the bottom water as the end product $N_2$ undergoes no further oxidation.

References list: my name is twice misspelled: Arndt et al. reference and Soetaert et al. reference.
We are sorry for the mistake and corrected the spelling. Other references were added.

Table 2: please check your reactions: R6 is unbalanced and its effect on TA, saturation degree, DIC etc is not mentioned

The equation has been balanced and the effects on TA, DIC and Ω have been added:

| R6 | Manganese oxidation | $2Mn^{2+} + O_2 + 4HCO_3^- \rightarrow 2MnO_2 + 4CO_2 + 2H_2O$ | -4/0 | - | - |

Also R15 has an effect on pH but that is complex function of pH (see Soetaert et al. 2007).

In effect, R15 drives pH towards the value of 7.9. So we precised:

| R15 | Anaerobic methane oxidation | $CH_4 + SO_4^{2-} \rightarrow HS^- + HCO_3^- + H_2O$ | 2/1 | + (if pH < 7.9) | + |

**Manuscript revision (doi:10.5194/bg-2016-212): Responses to the referees' comments:**

We thank the reviewer for his helpful and constructive comments. In the following document, we answer the questions (in black) one by one in blue. Modifications that have been done in to the manuscript are written in *italics*.

**Reviewer #1** D. Burdige (Referee)

Unfortunately, the discussion of the results is too general and poorly focused. Overall I think much more could be done with the data. Much of the data interpretation is too speculative or is simply based on comparisons with what other workers have seen in these (and other) sediments. In many places the text reads more like a data report interspersed with comments about similarities between these results and results from other studies. The things that are new and exciting and different about this work, as compared to these other studies, are not clearly presented.

In the reviewed version, we focus more on the new findings of our work. For this area, we present the first data set containing at once pore water concentrations of DIC, TA and microprofiles of oxygen and pH in order to deal with carbonate dissolution/precipitation in these delta sediments. But as diagenetic processes are very complex, we were not able to measure all parameters. For this reason, sometimes we have no other choice than to rely on literature data and hypothesis.
Concerning the importance of the presented work, the following sentences have been added to the abstract (line 29):

*The large production of pore water alkalinity characterizes these sediments as an alkalinity source to the water column which may increase the $CO_2$ buffering capacity of these coastal waters. Estuarine sediments should receive more attention in future estimations of global carbon fluxes.*

To differentiate our work from previous studies, we added a couple of lines in the introduction (line 94):

*Previous studies in this region often focused on organic matter mineralization pathways measurements in the oxic sediment layers and analysis of particulate carbon (Lansard et al., 2008; Cathalot et al., 2010) or could not provide simultaneous DIC and TA pore water measurements (Pastor et al., 2011a). These studies did not provide information on TA production and fluxes at the SWI. Accordingly, we designed a study to investigate the interaction of mineralization processes on porewater pH and the fate of solid calcium carbonates. For that purpose, we used a combination of in situ oxygen and pH microelectrode measurements and pore water analysis of DIC, TA, $SO_4^{2-}$ and $Ca^{2+}$ concentrations to examine various diagenetic pathways on different vertical scales.*

Questions about whether sediments such as these are alkalinity sources is an important one, and the authors note this in places in the text. While they do have some discussions of their results with such considerations in mind, the discussions are rather disjointed. At a bare minimum, Fig. 5 shows that all of these sediments are a source of alkalinity to the water column, although this simple observation seemed (at least to me) to get lost in the overall discussion. I would urge the authors to re-structure the paper so that this general topic is much more clearly examined with their data. In my opinion, this will make this paper one that people will want to read (and should read).

Indeed this question is very important and we modified the text to focus the article more in this direction. To better introduce this question, we added in the introduction (line 44) ... :

*Anaerobic reactions also lead to production of total alkalinity (TA) that increases the $CO_2$ buffer capacity of seawater (Thomas et al., 2009). Variations in DIC and TA affect the partial pressure of $CO_2$ ($pCO_2$) in seawater and ultimately the $CO_2$ exchange with the atmosphere (Emerson and Hedges, 2008). By increasing the $CO_2$ buffer capacity of seawater, the release of TA from anaerobic sediments into the water column could account for a majority of the $CO_2$ uptake in shelf regions and deliver as much TA to the oceans as is derived from rivers (Thomas et al., 2009). Due to high dynamics, spatial heterogeneity and complex biogeochemical mechanisms, estimations of TA fluxes from the sediments are affected by high uncertainties (Krummins et al., 2013).*

... and discussed more explicitly in new paragraph between lines 325 and 326:

*In the Rhône River delta sediments, OM mineralization leads to DIC production, and under anoxic conditions, also to TA production. Our results demonstrate strong DIC and TA pore water gradients in the anoxic layer of the sediments indicating high anaerobic respiration rates. As a result, DIC and TA diffuse towards the SWI. No oxic reaction consumes DIC except potential carbonate precipitation. Our results indicate that more DIC is produced in the sediments than consumed by precipitation of $CaCO_3$. This means, that OM mineralization in the sediments leads to strong DIC fluxes from the sediments into the water column. For TA, the situation is more complicated, as oxidation of reduced species can consume as much TA as has been produced to reduce these species (Table 2). In a 1D system, where no precipitation occurs and no reduced species can be exported, 100% of the anaerobic TA would be consumed in the oxic layer.*
*Krumins et al., (2013) reported that the effective TA flux from the sediments into the water column is far less important than the anaerobic TA production due to the TA loss in the oxic layer. Unfortunately, the resolution of the DIC and TA pore water profiles in this current study does not give precise information about the gradients in the oxic layer. Thus, we can only speculate about the oxic TA consumption in this region and related TA fluxes across the SWI. According to (Pastor et al., 2011a), 97 % of the reduced species precipitate in the anoxic sediments in the Rhône prodelta. Therefore, the majority of the produced TA is likely released into the water column which can counterbalance the effects of the DIC fluxes and increase the $CO_2$ buffer capacity of the overlaying waters.*

and rephrased from line 455 to the end :

*As the alkalinity fluxes produced by anaerobic processes are high and likely not much reduced by reoxidation of reduced species in the oxic layer due to iron sulfide precipitation, net TA fluxes of the same order of magnitude than DIC fluxes are likely to occur. Therefore, the alkalinity build up in the anoxic zone could diffuse across the oxic sediment layer and contribute to buffer bottom waters and increase $CO_2$ storage capacity of these waters. The large precipitation of calcium carbonate in the proximal zone may have implications for the $CO_2$ source potential from the sediment. Indeed, calcium carbonate precipitation generates $CO_2$ (R2b) which can then be exported to the water column. In addition, calcium carbonate precipitation consumes TA. However, the order of magnitude of the TA consumption by carbonate precipitation in these sediments is below the quantity of TA produced by sulfate reduction. Without this TA flux, the $pCO_2$ of the bottom waters in the prodelta of the Rhône would likely be much higher than observed.*

In order to make sure if these sediments are important alkalinity sources or if the majority of the anaerobically produced TA is consumed in the oxic sediment layer, we carried out in situ flux

measurements together with Martial Taillefert and Eryn Eitel in September 2015. The data wich are still beeing processed will be published in a separate paper.

Before final publication the manuscript will need to be carefully copy-edited by a native or fluent English-speaker. There are many places where there are grammatical errors, awkward syntax, and curious phrasings.

The manuscript was copy-edited by a native English-speaker (Patrick Laceby, LSCE)

One last general comment. When I read lines 91-94 and the sentence starting at the end of line 124 ("The sea floor in this region : : :") I had the sense that these sediments have some degree of similarity to those of other large river deltas like, e.g., the Amazon (see, for example, Aller's 1998 Marine Chemistry paper cited here). In contrast, much of the discussion of the data in the text takes a very traditional, steady-state "Froelich et al."-type approach (see, for example, section 2.7 and much of section 4.1). To me, this approach seems to contradict the text on lines 91-94 and 124, and I think that some clarification is needed.

Indeed, this environment is very dynamic, but very different from the Amazon delta due to the lack of tidal mixing and strong permanent currents. The prodelta of the Rhône is dominated by very high accumulation rates due to flood depositions and resuspension events during winter stroms can remove several centimeters of sediment. Despite this fact, molecular diffusion is the dominant transport process and we find the same general tendencies from cruise to cruise.

We added a sentence to the description of the sampling site to point at the particularity of this environment at line 92 and rephrased:

*The "predominance" of sediment accumulation over other dynamic processes and the absence of tidal mixing and dominant marine currents differentiate the prodelta of the Rhône differs from other deltaic environments like the Amazon, where the surface sediments are constantly reworked (Aller et al., 1998).*

To discuss different transport mechanisms, we added at the end of the section 4.1 (line 387) :

*Finding this clear succession of reactions is interesting, particularly the pH profiles that look classical in the aerobic sediment layers sampled from this complex and dynamics system. As OPDs measure only a couple of mm, molecular diffusion is by far the dominant transport process (Peclet number $\gg 1$ on a scale of the OPD). The microstructure of these sediments is restored very fast after distrubances like resuspension events (Toussaint et al., 2014). Furthermore, the comparison with previous studies shows, that despite the high sediment dynamics in this region, the general biogeochemical tendencies are maintained throughout time.*

and added a new reference:
*Toussaint F., Rabouille, C., Cathalot, C., Bombled, B., Abchiche, A., Aouji, O., Buchholtz, G., Clemençon, A., Geyskens, N., Répécaud, M., Pairaud, I., Verney, R. and Tisnérat-Laborde, N.: A new device to follow temporal variations of oxygen demand in deltaic sediments: the LSCE benthic station, Limnol. Oceanogr.: Methods, 12, 729-741, 2014*


Specific Comments (line numbers in parentheses)

(215) I never realized there were 12 parameters of the carbonate system. Is this a typo or am I missing something?

Sorry, there are 9  parameters, the mistake has been corrected.

(225) Here and on line 291 they talk about good agreement between measured and calculated pH values. It might be good to show this, and/or present some additional information like, e.g., the slope and r2 value of a scatter plot of the two pH's.

We added at line 292 :
*A linear relationship of the pH data measured with microelectrodes against calculated pH by CO2SYS shows a correlation with a slope of 1.01 +/- 0.02 and an r² = 0.7483 (graph not shown).*

We compared the pH values calculated from DIC and TA data with microelectrode data. As the porewaters represent an integration of a certain sediment zone, the average signal of the microelectrodes for the same zone was used. The size of the influenced zone was calculated following: Seeberg-Elverfeldt, J., Schlüter, M., Feseker, T., Kölling, M.: Rhizon sampling of porewaters near the sediment-water interface of aquatic systems; Limnology and Oceanography: Methods, 3, 361-371, 2005

Because we already include 10 figures, we did not include a figure showing the correlation.

(251) I would probably be good to list here what atmospheric pCO2 was at the time of sampling.

We added at line 251:

*During the sampling period, the Integrated Carbon Observation System (ICOS) station at Manosque (l'Observatoire de Haute Provence, https://icos-atc.lsce.ipsl.fr/?q=OHP) measured a pCO2 of 410 ppm. At most stations, $pCO_2$ was oversaturated compared to the atmosphere, with the lowest values calculated close to the river mouth at stations A and Z and the highest values calculated in the bottom waters at the shelf stations*

(265) The way the pH data is plotted makes it hard to see things like differences in inflection points for different regions. It might be helpful to break Fig. 4 up into 3 panels like Figs. 5 and 6. It might also be useful to similarly sub-divide Fig. 2 (O2 profiles) into 3 panels.

Figure 2 and Figure 4 were sub-divided into 3 panels.

(286) Are these slopes statistically different in the three different regions? If not I would not report them separately but would simply list an overall slope for all of the sediments.

We changed the corresponding sentence at line 286 into:
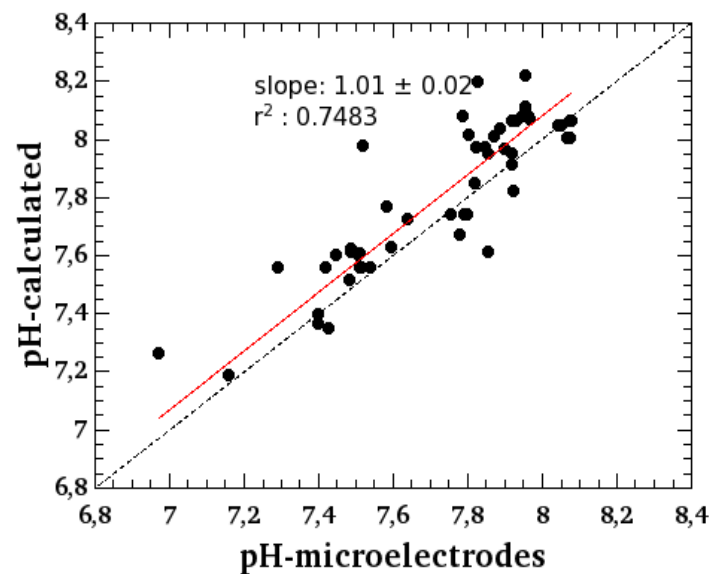
*The DIC and TA pore water profiles are well correlated in each core and the concentrations show a linear correlation with a slope of 1.01 and an $r^2$ = 0.9982 (130 data points).*

(317 -) Plotting sulfate concentrations and carbonate saturation state for each region on the same panels is very confusing. I would recommend separating them.

The figure in question was subdivided into two figures showing sulfate profiles and saturation states separately.

(405-) I would think that all of the things discussed here (organic matter oxidation state, carbonate precipitation, AOM) would affect the magnitude of the slope of a DIC/Sulfate plot, and not the scatter around the best-fit line. I'm also surprised that the slope is 2 despite all of these factors. Maybe they act (somehow) in such a way as to cancel each other out?

We changed the representation of the results into a $\Delta DIC$ vs $\Delta SO_4^{2-}$ plot that has a slope of 1.65. Taking into account the difference of the diffusion speed in sediments of these two species, we come close to a ratio of 2. Indeed, this is very surprising and we think that the processes in question cancel each other out. We rephrased the corresponding section in the discussion at line 400 to 409:

*To estimate the actual $\Delta DIC/\Delta SO_4^{2-}$ ratio due to diagenetic processes, the slope of the correlation between produced DIC ($\Delta DIC$) and consumed sulfates ($\Delta SO_4^{2-}$) in the pore waters (Fig 10) has to be corrected for molecular diffusion following the equation proposed by Berner (1980). Accordingly, we used the diffusion coefficients determined by Li and Gregory (1973). Below 10 cm depth, the observed diffusion corrected $\Delta DIC/\Delta SO_4^{2-}$ ratio equals 1.8 ± 0.02. The deviation of this measured value, from the theoretical value of 2 can be linked to higher oxidation states of organic matter which increases the $SO_4^{2-}$ requirement for DIC production (in an extreme case, if methane undergoes oxidation, the $\Delta DIC/\Delta SO_4^{2-}$ ratio equals 1), carbonate precipitation lowering DIC concentrations or methanogenesis that increases DIC without consuming $SO_4^{2-}$ (Burdige and Komada, 2011; Antler et al., 2014).*

*and further at line 417:*

*Despite all these divers reactions that affect the $\Delta DIC/\Delta SO_4^{2-}$ ratio, they are balanced in a way that $\Delta DIC$ and $\Delta SO_4^{2-}$ correlate well and do not show a deviation in the slope throughout the whole sediment depth investigated (Figure 10).*

(473) I don't see any direct evidence in the paper that terrestrial organic matter is what is being degraded. It might be, but without evidence to support this I would not be so definitive.

The sentence in question was rephrased:
*This confirms that the biogeochemistry in the prodelta region is driven by the import and processing of material from the Rhône River (Cathalot et al., 2010, 2013).*

Furthermore, different studies showed, that the majority of the sediment fraction in the proximal domain is land derived. This fraction decreases in offshore direction. During the DICASE cruise, porewater was sampled for analysis of $\delta^{13}C$ and $\Delta^{14}C$ signatures of porewater DIC in order to evaluate what OM fraction actually undergoes mineralization. The results point in the direction, that land

derived material is the DIC source in the pore waters close to the river mouth. An article to publish these results is on its way.

**Manuscript revision (doi:10.5194/bg-2016-212): Responses to the referees' comments:**

We thank the reviewer for his helpful and constructive comments. In the following document, we answer the questions (in black) one by one in blue. Modifications that have been done in to the manuscript are written in *italics*.

**Reviewer #2**

All minor comments of Reviewer #2 were taken into account.

Rassmann and collaborators present a very nice dataset of sediment properties in the Rhône river delta. Based on direct (microelectrodes) measurements of pH and O2 and on pore-water analyses of DIC, TA, Ca2+ and SO42- along a gradient from the river mouth to the open Mediterranean Sea (3 domains considered), this manuscript aims to describe and understand the main diagenetic reactions that control these sediment properties and the impact of the sediment on the bottom water carbonate chemistry. I would recommend publication of this manuscript following the proposed minor modifications and an extensive copy-edition by a native speaker.

The manuscript was copy-edited by a native English-speaker (Patrick Laceby, LSCE)

Table 2 and Section 2.7 should not be presented in the Material and Methods section but more likely in the Discussion.

We moved Section 2.7 to the beginning of the discussion and rephrased it.

I do not believe CO2 dissolution should be presented as a diagenetic reaction.
Table 2 should be made much clearer and for instance updated by: 1) providing the full name of the presented reactions, 2) dividing into 3 parts with reactions occurring in the presence of oxygen (oxic mineralization and reoxidation of reduced species), in the anoxic section (anaerobic mineralization and precipitation of reduced species), and both: CaCO3 dissolution or precipitation. Reaction R2, it is not clear whether you present CaCO3 dissolution or precipitation or both. I would consider 2 lines, one for precipitation, and one for dissolution as their effects on TA, DIC, pH and Omega are opposite. Finally, I would move this reaction to the end of the table (see above).

We sub-divided Table 2 into the 3 suggested categories and split reaction 2 into two lines for dissolution and precipitation.

Why don't you show nitrate reduction? This can be in some cases an important pathway.

Waters of the Northwest Mediterranean Sea show low nitrate concentrations. Only a minor part of OM is mineralized by this pathway in the study area. Nevertheless, denitrification has been added to the reaction table. To justify not to discuss nitrate reduction in this area, we cite (Pastor, L., Cathalot, C., Deflandre, B., Viollier, E., Soetaert, K., Meysmann, F.J.R., Ulses, C., Metzger, E. and Rabouille, C.: Modeling biogeochemical processes in sediments from the Rhône River prodelta area (NW Mediterranean Sea), Biogeosciences, 8, 1351-1366, 2011a.) at line 387:

*In contrast to other nearshore environments, nitrate reduction has been shown to account only for 2-5*

All reactions should be presented considering the same amount of OM mineralized (in some cases you have 1 or 2 moles of CH2O mineralized).

The stoichiometric coefficients in table 2 have been adjusted to 1 mol of $CH_2O$.

Figure 6 should be updated. First, you don't show the same Y-axis scale than on Figure 5, why is that? and furthermore, this scale in not the same between the 3 domains in this Figure 7.

We adjusted the scale on all figures to 40 cm depth.

I am a bit surprised by the very high heterogeneity that you found between stations in the Proximal domain and believe there are a number of mistakes to correct. For instance, you have DIC and TA data for station Z' until 30cm while you calculate pH up to 25. For station A', you seem to have DIC/TA data down to 25 cm and you calculate pH data down to 35 cm or more. Please check.

In effect, the area is highly heterogeneous, differences of 10 mmol/L in DIC or TA pore water concentrations at a same station in a certain depth are definitely possible.
We checked the figures for consistency. Indeed, some data points had disappeared on the graphs and were re-introduced.

Furthermore, I have calculated pH for station Z at the last sampled depth (between 20 and 25 cm) considering TA of 48 and DIC of 50 mmol/L, I end up with a pH of 7.18, far from the 7.8 shown in Figure 6. Again, this should be carefully checked.

We use CO2SYS with the thermodynamic constants from (Lueker, T. J., Dickson, A. G., Keeling, C. D.: Ocean $pCO_2$ calculated from dissolved inorganic carbon, alkalinity, and equations for $K_1$ and $K_2$ : validation based on laboratory measurements of $CO_2$ in gas and seawater at equilibrium, Mar. Chem., 70, 105-119, 2000.) with TP = 0.1 µmol/kg and TSi = 6.4 µmol/kg (Denis, L., Grenz, C.: Spatial variability in oxygen and nutrient fluxes at the sediment-water interface on the continental shelf in the Gulf of Lions (NW Mediterranean), Oceanologica Acta, 26, 373-389, 2003) and making the hypothesis that theses values are constant with depth (in lack of better data). Furthermore, we use the bottom water salinity of 37.5 and the in situ temperature of 16.0 °C. The water depth at this station is 18 m. The analysis has been done at a temperature of 25 °C.

For the data point cited:
Z(18cm): TA = 46.215 ± 0.474 mmol/kg, DIC = 45.440 ± 0.190 mmol/kg leads to  pH= 7.636 ± 0.059
Z(22cm): TA = 49.189 ± 0.504 mmol/kg, DIC = 47.363 ± 0.129  mmol/kg leads to  pH= 7.801 ± 0.048
and
Z(26cm): TA = 44.514 ± 0.484  mmol/kg, DIC= 44.506 ± 0.051 mmol/kg leads to pH=7.492  ± 0.051

If the discrepancies of your and our calculations persist, we should do a more detailed comparison of our methods with a whole dataset.

 L284-287:

You should present the determination coefficients and the corresponding slopes for each domain separately.

As the slopes were not significantly different, we followed the suggestion of Reviewer #1 and reported the overall slope 1.01 with $r^2 = 0.9982$.

L291: I would really like to see a more detailed comparison between measured and calculated pH.
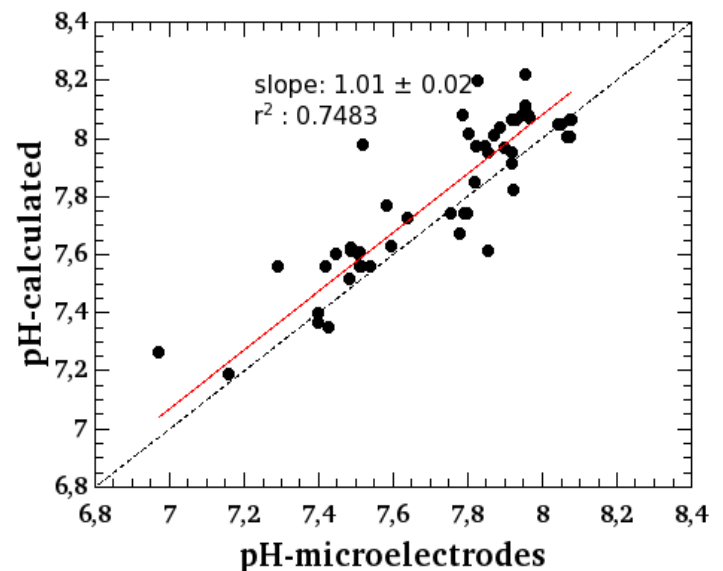
As already posted in the answer to Reviewer #1:

We added at line 292 :
*A linear relationship of the pH data measured with microelectrodes against calculated pH by CO2SYS shows a correlation with a slope of 1.01 +/- 0.02 and an $r^2$ = 0.7483 (graph not shown).*

We compared the pH values calculated from DIC and TA data with microelectrode data. As the porewaters represent an integration of a certain sediment zone, the average signal of the microelectrodes for the same zone was used. The size of the influenced zone was calculated following: Seeberg-Elverfeldt, J., Schlüter, M., Feseker, T., Kölling, M.: Rhizon sampling of porewaters near the sediment-water interface of aquatic systems; Limnology and Oceanography: Methods, 3, 361-371, 2005

Because we already include 10 figures, we did not include a figure showing the correlation.



Section 3.4. Why all stations are not shown for Ca2+ (D, A' and Z' missing), why 3 datasets for A ?

We do not have any data for stations D and Z'. In fact, there has been a confusion at station A: the data sets are from A and A' and a longer core at station A that has been removed in the reviewed version of the paper.

L43: This is not correct, following your Table 2, aerobic mineralization does not produce TA.

We rephrased:

*Aerobic and anaerobic reaction pathways contribute to the production of dissolved inorganic carbon (DIC), which creates acidification of the bottom waters. Anaerobic reactions lead as well to production of total alkalinity (TA)*

L152: I don' understand what is "the slope of the pH variation", please rephrase.

We rephrased:

*The calibration of the pH electrodes was carried out using NBS buffers, thus allowing the estimation of*

*the slope of the electrode signal in fonction of pH variation at onboard temperature. The slope was then recalculated at in situ temperature and the electrode signal variation was transformed into pH changes.*

L156: .. "using this BW value the micro electrode measured pH variations", please rephrase

We rephrased:

*The pH of bottom waters was determined using the spectrophotometric method with m-cresol purple following Clayton and Byrne, (1993) and Dickson et al., (2007). Pore water pH on the total proton scale ($pH_t$) was recalculated using the signal of the microelectrode adjusted to this BW value.*

L162: surface of 109 cm, this is not a surface.

The surface of the head of the moving unit of the lander, where the electrodes are mounted measures 109 cm²

L171: according to Broecker and Peng (1974) L180 to 191: please precise how many replicates were measured for each parameter (pH, O2, DIC and TA)

*All bottom water concentrations were measured as triplicates. Small sample volumes in pore waters only allowed for replicates for the DIC, $SO_4^{2-}$ and $Ca^{2+}$ analysis.*

L299: (Fig. 5) L313: > 95% calcite + >5 % Mg-calcite do not leave much room for aragonite: : :.

Yes, indeed, we did not detect any aragonite in this area. The drainage basin of the Rhône River is characterized by old carbonates and the calcifying organisms on site (foraminifers) produce calcite tests. There are no corals in this area.

In lack of better material, the aragonite standard used for the calibration of the X-ray analysis is natural coral powder, characterized to have less than 2 % of Ca content. (Kindler, P., Reyss, J.-L., Cazala, C., Plagnes V.: Discovery of a composite reefal terrace of middle and late Pleisocene age in Great Inagua Island, Bahamas. Implications for regional tectonics and sea-level history, Sedimentary Geology, 194, 141-147, 2007). It's diffraction analysis gives the following diffractogramme with the clearly visible principal Ar peak at $2\theta = 26.297°$ and its secondary peak at 27.298° (both slightly shifted from the theoretical value) :
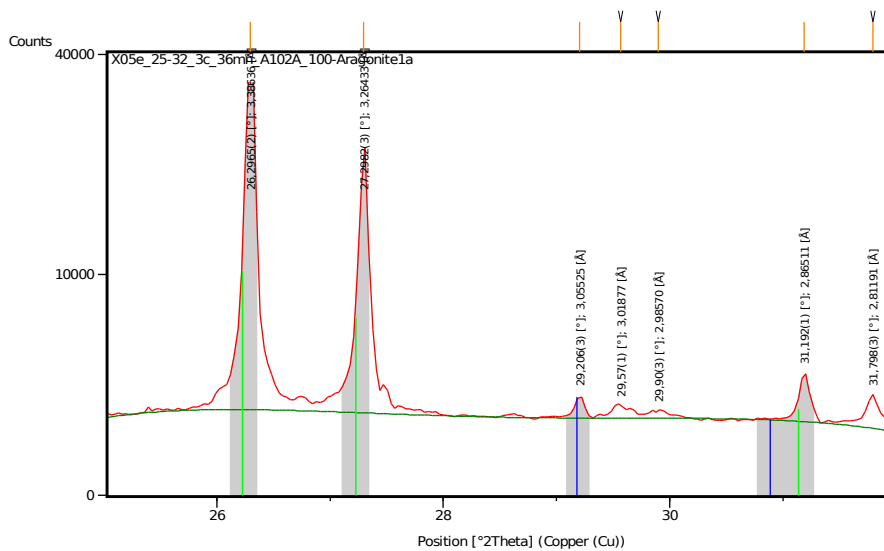
A typical diffractogramme of Rhone delta sediments looks like this (Station Z). We recognize clearly the principal calcite peak at 2θ = 29.468° with a little deformation at the right indicating the presence of magnesian calcite. The position of the aragonite peak is covered by the base of another peak at 2θ = 26.674. These diffractogrammes do not allow a better deconvolution of the peaks and we have an uncertainty about the material used to calibrate our DRX measurements. So the presence of aragonite cannot be completely excluded, but is unlikely.
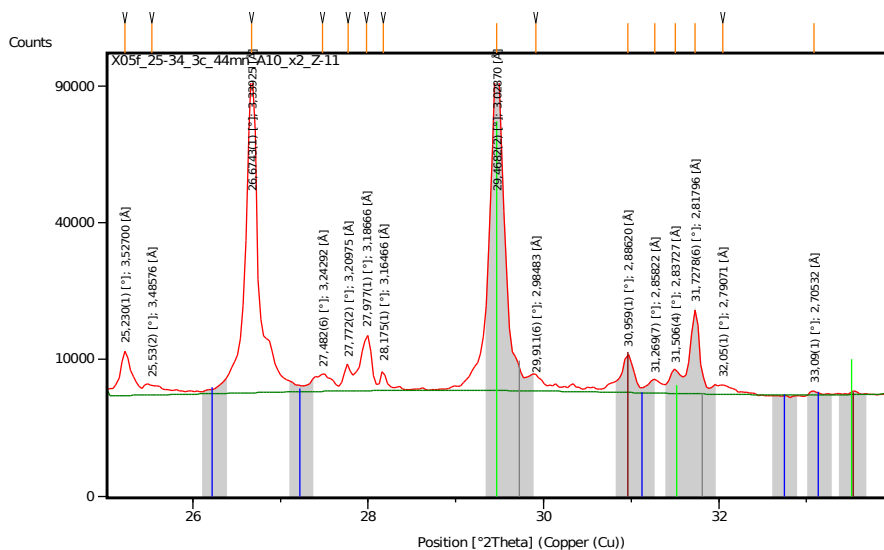


Many grammatical and formatting errors in the Discussion.

Grammatical and formatting errors have been corrected.

All figures starting from Figure 2: Average OPD for each domain should be shown on these plots.

The vertical scale on figures 2 and 4 is in mm whereas the vertical scale on the following figures is given in cm. The average OPD for each domain is situated between the sediment water interface and the first scale trait, so it would be invisible on these figures.

Figure 2 legend: in situ in italics Figure 3 legend: what do the vertical error bars correspond to? Please add.

We added in the legend of the figure:

*Error bars are standard deviations between the diffusive fluxes calculated from the 5 single oxygen profiles measured at each station.*

Figures 5 and 7: I would use the same x-axis scale for all 3 domains

We decided not to use the same concentration scale because the gradients are very different. Adjusting the scale for all figures would hide the form of the profiles in the prodelta and distal domain. To alert the reader about difference between the three concentration scales, we added to the figure caption:

*For better visibility of the profiles in each domain, the scale of the concentrations has been individually adjusted for each domain.*

and for Figure 7
separate SO42- and Omega, consider using 2 figures. On Figure 7, please note that the legend box hides the axis, which should be avoided.

The figure has been split into individual figures for sulfate concentrations and calcium carbonate saturation states.

Figure 6 and 7, and legends: what do the horizontal error bars correspond to? Please add.

We added to the caption of figure 6:

*The error bars are estimations of the error propagation from the measured data in the calculation.*

and to the caption of figure 7:

*The error bars represent the uncertainties of the ICP-AES measurement.*

# Carbonate chemistry in sediment pore waters of the Rhône River delta driven by early diagenesis (NW Mediterranean)

Jens Rassmann[1], Bruno Lansard[1], Lara Pozzato[1,2], Christophe Rabouille[1]

[1]Laboratoire des Sciences du Climat et de l'Environnement, LSCE/IPSL, CEA-CNRS-UVSQ-Université Paris Saclay, Gif-sur-Yvette, 91198, France

[2]Institut Méditerranéen d'Océanologie, CNRS-IRD-Université de Toulon-Aix Marseille, 13288 France

*Corresponding author*: Jens Rassmann (jens.rassmann@lsce.ipsl.fr)

**Abstract.** The Rhône River is the largest source of terrestrial organic and inorganic carbon for the Mediterranean Sea. A large fraction of this terrestrial carbon is either buried or mineralized in the sediments close to the river mouth. This mineralization follows aerobic and anaerobic pathways with a range of impacts on calcium carbonate precipitation and dissolution in the sediment near the sediment-water interface. This study focuses on the production of dissolved inorganic carbon (DIC) and total alkalinity (TA) by early diagenesis, consequential pH variations and the effect on calcium carbonate precipitation or dissolution. The sediment pore-water chemistry was investigated along a transect from the Rhône River outlet to the continental shelf. TA and concentrations of DIC, $SO_4^{2-}$ and $Ca^{2+}$ were analyzed on bottom waters and extracted sediment pore waters, whereas pH and oxygen concentrations were measured *in situ* using microelectrodes. The average oxygen penetration depth into the sediment was $1.7 \pm 0.4$ mm close to the river mouth and $8.2 \pm 2.6$ mm in the continental shelf sediments, indicating intense respiration rates. Diffusive oxygen fluxes through the sediment-water interface ranged between 3 and 13 mmol $O_2$ $m^{-2}$ $d^{-1}$. In the first 30 cm of the sediment, TA and DIC pore water concentrations increased with depth up to 48 mmol $L^{-1}$ near the river outlet and up to 7 mmol $L^{-1}$ on the shelf as a result of aerobic and anaerobic mineralization processes. Due to aerobic processes, at all stations pH decreased by 0.6 pH units in the oxic layer of the sediment accompanied by a decrease of the saturation state regarding calcium carbonate. In the anoxic layer of the sediments, sulfate reduction was the dominant mineralization process and was associated to an increase of pore water saturation state regarding calcium carbonate. Ultimately anoxic mineralization of organic matter caused calcium carbonate precipitation demonstrated by a large decrease in $Ca^{2+}$ concentration with depth in the sediment. Carbonate precipitation decreased in the offshore direction, together with the carbon turnover and sulfate consumption in the sediments. The large production of pore water alkalinity characterizes these sediments as an alkalinity source to the water column which may increase the $CO_2$ buffering capacity of these coastal waters. Estuarine sediments should therefore receive more attention in future estimations of global carbon fluxes.

1

# 1 Introduction

The coastal ocean is a net sink of atmospheric $CO_2$ and plays an important role in the global carbon cycle (Hedges and Keil, 1995; Chen and Borgès, 2009; Bauer et al., 2013; Laruelle et al., 2013). This dynamic region is not only a sink for atmospheric $CO_2$, but also a location where terrestrial organic and inorganic carbon is buried or recycled (Hedges and Keil, 1995; Cai, 2011). Due to strong pelagic-benthic coupling, a large fraction of organic matter (OM) is mineralized in continental shelf sediments (McKee et al., 2004; Burdige, 2011; Bauer et al., 2013). Estuaries and deltas are a very dynamic part of coastal ocean regions, characterized by high carbon turnover (Hedges and Keil, 1995; Cai, 2011). They are the principal link between continents and oceans and receive inputs of terrestrial organic and inorganic carbon, in both, particulate and dissolved phases (McKee et al., 2004; Cai, 2011; Dai et al., 2012; Bauer et al., 2013). An important fraction of these inputs remains on site and undergoes oxic and anoxic mineralization (Andersson et al., 2005; Aller and Blair, 2006; Chen et al., 2012). Despite their importance for the coastal carbon cycle, there is a lack of knowledge about the links between early diagenesis and the carbonate system in river dominated sediments (McKee et al., 2004).

Aerobic and anaerobic reaction pathways contribute to the production of dissolved inorganic carbon (DIC) resulting in the acidification of the bottom waters. Anaerobic reactions also lead to production of total alkalinity (TA) that increases the $CO_2$ buffer capacity of seawater (Thomas et al., 2009). Variations in DIC and TA affect the partial pressure of $CO_2$ ($pCO_2$) in seawater and ultimately the $CO_2$ exchange with the atmosphere (Emerson and Hedges, 2008). By increasing the $CO_2$ buffer capacity of seawater, the release of TA from anaerobic sediments into the water column could account for a majority of the $CO_2$ uptake in shelf regions and deliver as much TA to the oceans as is derived from rivers (Thomas et al., 2009). Due to high dynamics, spatial heterogeneity and complex biogeochemical mechanisms, estimations of TA fluxes from the sediments are affected by high uncertainties (Krummins et al., 2013). The processes by which TA is produced in the sediments are still not well understood. Anaerobic respiration (e.g. denitrification, sulfate reduction, iron and manganese reduction) may play a major role, although dissolution/precipitation of calcium carbonate may also have a large impact on TA concentrations (Jahnke et al., 1997; Thomas et al., 2009, Krumins et al., 2013). Indeed, the changes in sediment pore water composition and pH can lead to over or under saturation of the calcium carbonate saturation state ($\Omega$), and therefore influence carbonate dissolution and burial in sediments. Furthermore, carbonate dissolution was correlated to alkalinity fluxes across the sediment-water interface (SWI) (Mucci et al., 2000).

Using *in situ* microelectrode measurements, Komada et al. (1998) and Cai et al. (2000) investigated small scale changes in $pCO_2$, pH and DIC in deep marine sediments and the exchange fluxes associated. In continental shelf sediments, Mucci et al. (2000) found that oxic mineralization can induce carbonate

2

dissolution below the sediment-water interface, extending the observations of Jahnke et al., (1997, 2004) to coastal sediments. Burdige et al., (2008, 2010) pointed out that carbonate dissolution is also driven by oxic respiration in the shallow carbonated sediments of the Bahamas Bank. Concerning anoxic processes, Van Capellen and Wang (1996) demonstrated that high manganese and iron contents in the sediments of the Skagerrak (Eastern North Sea) and associated OM mineralization can increase pore water pH by proton-consuming reduction processes of oxidized iron and manganese. These authors, with Froelich et al. (1979) and Berner (1980) as precursors, highlighted the complexity of the multiple competing reaction pathways in anoxic sediment.

In regions with a high carbon turnover, sulfate reduction is a large contributor to anoxic early diagenesis and can even be the dominant mineralization process for OM (Mucci et al., 2000; Burdige and Komada, 2011; Pastor et al., 2011). Sulfate reduction slightly decreases pH (Jourabchi et al, 2005; Soetaert et al., 2007), but nevertheless, it tends to enhance carbonate precipitation because of its coupling with precipitation of sulfide minerals from iron oxides (Gaillard et al., 1989; Mucci et al., 2000; Burdige, 2011). As an example, in sapropelic sediments from a Mangrove Lake, Mackenzie et al. (1995) reported a stable pH throughout the sulfate-reduction zone and a buildup of supersaturation with respect to carbonate with depth. These results contrast with the theoretical perspective that sulfate reduction was supposed to lead to carbonate dissolution because of the pH decrease (Jourabchi et al., 2005). Even today, the reproduction of measured pore water profiles in the sediments and the estimation of TA and DIC fluxes across the SWI by modeling are very challenging (Arndt et al., 2013; Krumins et al., 2013; Jourabchi et al., 2005). In addition, the magnitude of DIC and TA fluxes across the SWI are not well constrained and can vary significantly between different study sites (Mucci et al., 2000).

The objective of this study is to improve our understanding of the influence of early diagenesis of organic matter on carbonate dissolution and precipitation, and the production of DIC and TA. Therefore, we collected seawater and sediment samples along a transect from the Rhône River delta to the Mediterranean Sea continental shelf covering a broad range of biogeochemical characteristics (Lansard et al., 2008; Cathalot et al., 2010; Cathalot et al. 2013). The Rhône River delta receives inputs of terrestrial organic and inorganic carbon, in both particulate and dissolved phases which decrease with the distance to the river mouth. The majority of these inputs remains on site and undergo mineralization in the sediments (Pastor et al., 2011a). Therefore sediments display strong spatial gradients in biogeochemical parameters such as nutrients, organic and inorganic carbon, affecting the diagenetic transport-reaction network (Bourgeois et al., 2011; Lansard et al., 2009). High sedimentation rates and resuspension events make this environment very dynamic and heterogeneous (Cathalot et al., 2010). The "predominance" of sediment accumulation over other dynamic processes and the absence of tidal mixing and dominant marine currents differentiate the prodelta of the Rhône from other deltaic environments like the Amazon, where the surface sediments are constantly reworked (Aller et al.,

3

Previous studies in this region often focused on organic matter mineralization pathways measurements in the oxic sediment layers and analysis of particulate carbon (Lansard et al., 2008; Cathalot et al., 2010) or could not provide simultaneous DIC and TA pore water measurements (Pastor et al., 2011a). These studies did not provide information on TA production and fluxes at the SWI. Accordingly, we designed a study to investigate the interaction of mineralization processes on pore water pH and the fate of solid calcium carbonates. For that purpose, we used a combination of i*n situ* oxygen and pH microelectrode measurements and pore water analysis of DIC, TA, $SO_4^{2-}$ and $Ca^{2+}$ concentrations to examine various diagenetic pathways on different vertical scales. We investigated a transect of stations characterized by various biogeochemical conditions (from oxic-dominated to sulfate reduction-dominated sediments). Furthermore, we calculated and discussed the calcium carbonate saturation state in regards to the different intensity of biogeochemical processes in these river-dominated sediments and estimated how early diagenesis impacts the bottom water carbonate chemistry (DIC, TA and $pCO_2$).

## 2 Study site and methods

### 2.1 The Rhône River delta

With a drainage basin of 97 800 $km^2$ and a mean water-discharge of 1700 $m^3$ $s^{-1}$, the Rhône River is the largest river of the Mediterranean Sea in terms of fresh water discharge, inputs of sediment and terrestrial organic and inorganic matter (Pont, 1997; Durrieu de Madron et al., 2000; Sempéré et al., 2000). The Rhône River mouth is a wave-dominated delta located in the microtidal Mediterranean environment of the Gulf of Lions (Sempéré et al., 2000). Its river plume is mostly oriented southwestward, due to the Coriolis Effect and the wind forcing (Estournel et al., 1997). The annual discharge of particulate inorganic carbon (PIC) is estimated to be 0.68 ± 0.45 $10^9$ gC $yr^{-1}$ (Sempéré et al., 2009). The total particulate organic carbon (POC) deposition in the Rhône delta system (265 $km^2$) is approximately 100 ± 31 $10^9$ gC $yr^{-1}$ with the deltaic front accounting for nearly 60 % of the total POC deposition (Lansard et al., 2009). In front of the river mouth, the deposited sediments are of a cohesive nature and composed of fine grained sediments (e.g. > 90 % silt and clay) (Roussiez et al., 2005; Lansard et al., 2007). Previous studies demonstrated that the carbonate content in the surface sediments varies between 28 and 38 % (Roussiez et al., 2006) and the content of organic carbon (OC) varies between 1 and 2 % (Roussiez et al., 2005, 2006; Lansard et al., 2008, 2009). The PIC in the sediments is composed by autochtonous and allochtonous carbonates with the most abundant calcifying organisms in this area being foraminifera (Mojtahid et al., 2010).

The seafloor bathymetry shows that the delta is divided in three zones, characterized by different water depth, sedimentation rate and strength of bathymetric slope. Got and Aloisi (1990) defined three major domains: the Proximal domain, in a radius of 2 km from the river outlet with water depth ranging from

4

10 to 30 m, the Prodelta domain, between 2 and 5 km from the river mouth with depth ranging from 30 to 70 m, and the Distal domain, with depth between 70 and 80 m passed the 5 km from the river mouth. Annual sedimentation rates reach up to 30-48 cm yr$^{-1}$ close to the river mouth (Charmasson et al., 1998) and rapidly decrease below 0.1 cm yr$^{-1}$ on the continental shelf (Miralles et al., 2005). The seafloor in this region is a dynamic environment based on sediment deposition and accumulation and with important heterogeneity regarding diagenetic activities, sediment pore water profiles and exchange fluxes at the sediment-water interface (Lansard et al., 2009; Cathalot et al., 2010). Diffusive oxygen fluxes into the sediment show spatial variability, both with the distance from the river mouth (decreasing in offshore direction) and on the horizontal scale of a few cm² (Lansard et al., 2009; Pastor et al., 2011b). Anoxic mineralization processes play a major role in the Prodelta sediments and are dominated by iron and sulfur cycling (Pastor et al., 2011a).

## 2.2 Sampling Stations

Ten stations have been sampled along the main direction of the Rhône River plume during the DICASE oceanographic cruise that took place in the Gulf of Lions between June 2-11, 2014 on board of the RV Tethys II (http://dx.doi.org/10.17600/14007100). The positions and main characteristics of the sampling stations are shown in Figure 1 and in Table 1. The stations were between 2 and 25 km distance from the Rhône River mouth, covering a bathymetric gradient ranging from 20 m to 80 m of water depth and representing the three different domains (A, Z : Proximal Domain; AK, B, K, L : Prodelta Domain and C, D, E, F : Distal Domain). The stations in the proximal domain A and Z have been sampled twice, in order to investigate spatial variability at these two stations. During this cruise, a benthic lander was used to measure *in situ* oxygen and pH micro profiles and sediment cores were taken for pore water extraction and solid phase analysis. The cruise took place during a period of low water discharge (957 m$^3$ s$^{-1}$) and air temperatures between 20 °C and 30 °C.

## 2.3 *In situ* measurements

To measure *in situ* oxygen and pH micro profiles at the sediment-water interface, an autonomous lander (Unisense®) was used. This lander is equipped with a high precision motor capable of simultaneously moving five oxygen microelectrodes (Revsbech, 1989), two pH microelectrodes and a resistivity probe (Andrews and Bennet, 1981) with a vertical resolution of 100 µm. The recorded oxygen profiles were calibrated using oxygen concentrations measured in bottom waters (BW) by Winkler Titration (Grasshoff et al., 1983) and the zero oxygen measured in the anoxic zone (Cai and Sayles, 1996). The SWI was positioned where the strongest vertical oxygen gradient was measured (Rabouille et al., 2003). The calibration of the pH electrodes was carried out using NBS buffers, thus allowing the estimation of the slope of the electrode signal in function of pH variation at onboard temperature. The slope was then recalculated at *in situ* temperature and the electrode signal variation was transformed into pH changes.

5

170 The pH of bottom waters was determined using the spectrophotometric method with m-cresol purple following Clayton and Byrne, (1993) and Dickson et al., (2007). Pore water pH on the total proton scale ($pH_t$) was recalculated using the signal of the microelectrode adjusted to this pH-BW value. At each depth, the profiler waited for 20 s to stabilize the electrode before measurements were recorded. Each data point is an average of five measurements carried out at every depth. For all *in situ* profiles,

175 the signal drift of each microelectrode was examined to ensure it was < 5 % from the beginning to the end of the measurements. The slope of the pH electrodes was double checked to make sure it was at least 95 % of the theoretical slope from the Nernst equation of -59 mV per pH-unit at 25 °C. At each station, 5 oxygen profiles and two pH profiles were measured simultaneously on a sediment surface of 109 cm².

180 **2.4 Calculation of oxygen fluxes across the sediment-water interface**

Sediment oxygen uptake rate has been widely used to assess benthic OC mineralization during early diagenesis. The total oxygen uptake (TOU) rate can be split into two parts: (i) the diffusive oxygen uptake rate (DOU), and (ii) the advective oxygen uptake. The DOU rates were calculated using Fick's first law (Berner, 1980):

185
$$DOU = -D_s \cdot \varphi \frac{d[O_2]}{dz}|z=0 \quad (1)$$

with:

$D_s$ : apparent diffusion coefficient adjusted for diffusion in porous environment calculated following

$$D_s = \frac{D_0}{1+3 \cdot (1-\varphi)}$$ where $D_0$ is the diffusion coefficient in free water according to (Broecker and Peng, 1974)

190 $\phi$ : sediment porosity

$$\frac{d[O_2]}{dz}|z=0$$ : Oxygen gradient at the sediment-water interface

**2.5 Sampling and *ex situ* measurements**

Bottom water samples were collected with a12-L Niskin bottle as close as possible to the seafloor at each station. For these samples, temperature was measured using a digital thermometer with a precision

195 of 0.1 °C and salinity was measured with a salinometer having a precision of 0.1. The pH, concentrations of DIC, TA and dissolved $O_2$ were measured on board within one hour for pH and within six hours for DIC and TA. The pH of seawater was measured using a spectrophotometer and m-cresol

purple as dye (Clayton and Byrne, 1993; Dickson et al., 2007) with uncertainties smaller than 0.01 pH units. Oxygen concentrations were determined using Winkler titration with an average uncertainty of 0.4 µmol L$^{-1}$. All DIC concentrations (bottom waters and pore waters) were measured on a DIC analyzer (Apollo SciTech®) using 1 ml sample volume with 4 to 6 replicates. The principle of the method is to acidify the sample with 10 % phosphoric acid to transform all forms of DIC into $CO_2$. The sample is then outgassed using ultra-pure nitrogen as a vector gas. The degassed $CO_2$ is quantified by a LICOR® gas analyzer, containing a non-dispersive infrared detector (NDIR). To calibrate the method, a certified reference material (CRM-batch #122, provided by A. Dickson, Scripps Institution of Oceanography) was used at least twice a day to confirm the accuracy of the DIC and TA measurements. TA concentrations were measured in a potentiometric open cell titration on 3 ml sample volume (Dickson et al., 2007). In our study, TA refers to total alkalinity, including silicates, phosphates, sulfides, organic alkalinity, etc.. The DIC and TA uncertainties in the sediment pore waters were below 0.5 %.

Sediment cores were sampled using an UWITEC® single corer (60 cm length, 9.5 cm inner diameter). After sampling, the cores were rapidly introduced in a glove bag with a $N_2$ atmosphere, to avoid oxidation, and pore waters were extracted using Rhizons, with pore size of 0.1-0.2 µm (Seeberg-Elverfeldt et al., 2005). The Rhizons had been degassed and stored in a $N_2$-filled gas tight box before use. Pore waters were extracted with a 2 cm vertical resolution and split into subsamples for DIC, TA, $SO_4^{2-}$ and $Ca^{2+}$ analysis. Sulfate concentrations were measured in the laboratory using a turbidimetric method (Tabatai, 1974). Concentrations of calcium ions were measured using ICP-AES (Ultima 2, Horiba®) by the "Pôle Spectométrie Océan" in Brest (France) with a relative uncertainty of 0.75 %. The calcium concentrations were salinity corrected by assuming constant $Na^+$ concentrations with depth in the pore water to avoid any evaporation effects due to sample storage. All bottom water concentrations were measured as triplicates. Small sample volumes in pore waters only allowed for replicates for the DIC, $SO_4^{2-}$ and $Ca^{2+}$ analysis but not for TA.

At each station, additional cores were taken for solid phase analysis. To establish porosity profiles, fresh sediment samples were weighed, dried for one week at 60 °C and weighed again. Knowing the salinity and density of seawater and sediment, porosity was calculated from the weight loss after drying. Total carbonate content of the solid phase was analyzed using a manocalcimeter with uncertainties of 2.5 % of $CaCO_3$. A manocalcimeter is a small, gastight container where the sediment can be acidified with HCl to dissolve calcium carbonates. The resulting increase of pressure is measured with a manometer and is directly proportional to the carbonate content of the sediment sample. Sediment samples have also been analyzed to quantify the calcite/aragonite proportion via X-Ray diffraction (XRD) on a X-Pert Pro diffractometer, using the θ-θ technique with the K-α-line of copper. The uncertainties of the XRD measurements were below 5 % of the aragonite proportion (Nouet and Bassinot, 2007).

7

## 2.6 Calculation of carbonate speciation, $CaCO_3$ saturation states and pH in pore waters

235    According to Orr et al. (2015), the best way to compute the 9 parameters of the carbonate system at *in situ* conditions is to start with DIC and TA concentrations. The thermodynamic constants proposed by Lueker et al. (2000) were used to calculate DIC speciation and pore water pH with the program CO2SYS (Lewis and Wallace, 1998). The calcium carbonate saturation state, for both calcite and aragonite, is expressed as the solubility product of calcium and carbonate ions concentrations divided by

240    their solubility constant $k_{sp}$:

$$\Omega_{Ca} = \frac{\left[Ca^{2+}\right]\left[CO_3^{2-}\right]}{k_{sp}} \quad (2)$$

The solubility constant $k_{sp}$ was calculated for *in situ* temperature, salinity and pressure following Millero et al. (1979), Mucci (1983) and Millero (1995).

## 3 Results

245    ### 3.1 Bottom waters

In June 2014, the Rhône River water discharge was low and close to 1000 $m^3$ $s^{-1}$ for the previous 2 months. Accordingly, the extent and thickness of the Rhône River plume were limited and bottom waters were not influenced by the river outflow, even close to the river mouth. Bottom water temperature, salinity, $O_2$, DIC, TA, pH, $SO_4^{2-}$ and $pCO_2$, are reported in Table 1. Salinity remained very

250    constant close to the seafloor, whereas temperature decreased with water depth from 16.8 to 14.3°C. Bottom waters were well oxygenated and oxygen concentrations decreased also with increasing water depth. DIC and TA concentrations varied slightly and the TA/DIC ratio in the bottom waters of all stations was $1.1 \pm 0.02$. The pH of bottom water was locally variable with a general decrease in offshore direction. $SO_4^{2-}$ concentrations were constant between the stations with typical values for seawater

255    around 30 mmol $L^{-1}$. During the sampling period, the Integrated Carbon Observation System (ICOS) station at Manosque (l'Observatoire de Haute Provence, https://icos-atc.lsce.ipsl.fr/?q=OHP) measured a $pCO_2$ of 410 ppm. At most stations, the bottom water $pCO_2$ was oversaturated compared to the atmosphere, with the lowest values calculated close to the river mouth (stations A and Z) and the highest values calculated at the shelf stations

260

### 3.2 The oxic layer

8

Figure 2 shows all oxygen profiles measured *in situ* during the DICASE cruise. The oxygen penetration depth (OPD) into the sediment was $1.7 \pm 0.4$ mm in the proximal domain, $3.3 \pm 1.3$ mm in the prodelta domain and $8.2 \pm 2.6$ mm in the distal domain. Some profiles had burrows creating small oxygen peaks below the OPD. The diffusive oxygen uptake rate (DOU) calculated from the measured oxygen profiles are plotted in Figure 3 as a function of the distance to the river mouth in the direction of the river plume. The positive value signifies an uptake of $O_2$ into the sediment. The DOU decreases exponentially with distance from $12.3 \pm 1.1$ mmol m$^{-2}$ d$^{-1}$ at station A towards the minimum flux of $3.8 \pm 0.9$ mmol m$^{-2}$ d$^{-1}$ at station F.

*In situ* pH micro profiles were measured in the top 4 cm of the sediment at all stations (Fig. 4). Immediately below the SWI, the pH decreases by 0.6 to 0.7 pH units in the oxic layer. Similarly to the oxygen micro profiles, the pH gradient in the OPD is stronger close to the river mouth and weaker in the distal domain. Just below the first drop, pH increases by 0.1-0.2 pH units and tends towards an asymptotic value between 7.4 to 7.6. The pH inflexion point, i.e. where the pH decrease stops and pH starts increasing, is located deeper in the distal zone than in the proximal zone, just below the OPD. Note that pH profiles show high spatial heterogeneity, even at one station.

## 3.3 DIC and TA pore water concentrations and calculated pH

Figure 5 shows the DIC and TA pore water profiles measured during the DICASE cruise. All pore water gradients across the sediment-water interface were strongest close to the river mouth and decreased in offshore direction. At the SWI, the DIC gradients were stronger than the TA gradients for all stations. Despite the spatial heterogeneity in the sediments, the three major areas defined by Got and Aloisi 1990) in this region display different biogeochemical gradients. Accordingly, stations from each group will be reported and discussed separately. In the proximal domain (stations A and Z), DIC concentrations and TA increase immediately below the SWI and reach a maximum value of 48 mmol L$^{-1}$ at 20 cm depth in the sediments, where the concentrations stabilize. In the prodelta domain (stations AK, B, K and L), DIC concentrations and TA increase to values of 5 mmol L$^{-1}$ in the first 10 to 15 cm depth. Below this depth, the gradients become stronger and DIC concentrations increase with TA up to 12 to 15 mmol L$^{-1}$ at the bottom of the cores (i.e. around 25 cm). This succession of two different gradient shapes in the TA and DIC profile is also observed in the distal domain (stations C, D, E and F), but the absolute values of the gradients are weaker. In the first 10 to 15 cm, the concentrations reach values of 3.5 mmol L$^{-1}$ and increase up to 5 to 7.5 mmol L$^{-1}$ at the bottom of the core. These very high DIC concentrations in the sediment are related to large DIC and TA gradients which are 4 to 10 times stronger in the proximal domain than at the other sites. The DIC and TA pore water profiles are well correlated in each core and the concentrations show a linear correlation with a slope of 1.01 and an $r^2 = 0.998$ (130 data points).

9

The sediment pH profiles were calculated from TA and DIC concentrations using CO2SYS. The pH is reported on the total proton scale ($pH_T$). In the first mm, the pH drops at all stations due to aerobic respiration (Figure 6). Below the oxygen penetration depth, the pH varies between 7.2 and 7.8 and converges towards the range of 7.4 to 7.6.

Existing numerical tools have been developed for the oxic water column. Nevertheless we used them in the sediments knowing that pore water concentrations (e.g. DIC, TA) are much larger than those in the water column and that reduced metabolites are unfortunately neglected. Despite this potential artifact, the calculated outputs (e.g. pH) agree with our measurements. A linear relationship of the pH data measured with microelectrodes against calculated pH by CO2SYS shows a correlation with a slope of 1.01 +/- 0.02 and an $r^2$ = 0.7483 (graph not shown).

## 3.4 Calcium and sulfate concentrations

At all stations, bottom water $Ca^{2+}$ concentration varies between 10 and 11 mmol $L^{-1}$ (Fig. 7). In the proximal domain, the $Ca^{2+}$ concentration decreases just below the SWI to reach a minimum of 2 mmol $L^{-1}$ at 15-20 cm depth, where DIC and TA concentrations reach a maximum and sulfate concentration a minimum. In the prodelta domain, the $Ca^{2+}$ concentration remains stable with depth until 10-15 cm in relation to the weaker TA and DIC gradients (Fig. 7). Below this depth, where the TA and DIC gradients increase, $Ca^{2+}$ decreases to values around 7 mmol $L^{-1}$ at the bottom of the cores. The distal domain is characterized by constant $Ca^{2+}$ concentrations which remain above 10 mmol $L^{-1}$ and the sulfate concentrations stay close to bottom water concentration.

In extracted sediment pore water, sulfate concentrations range from 5 to 32 mmol $L^{-1}$ from the surface down to 30 cm depth. Our measurements indicate strong sulfate consumption rates in the proximal domain (Fig. 8) where DIC and TA gradients are strong as well. In the proximal domain, sulfate concentration decreases in the first cm below the SWI compared to the bottom water. In the prodelta domain, sulfate reduction starts to occur between 10 and 15 cm depth, the same depth where TA and DIC gradients increase. In the distal domain, no significant sulfate reduction occurs in the first 30 cm, as sulfate concentration remains constant and TA and DIC gradients are low compared to the other domains.

## 3.5 Solid carbonates and calcium carbonate saturation state

The carbonate content of the solid phase scattered around 35 % at all stations, from the surface down to 30 cm. The composition of sedimentary $CaCO_3$ was dominated by calcite ($\approx$ 95 %), with a small fraction of magnesian calcite (< 5 %), and only traces of aragonite (data not shown). Accordingly, only $\Omega_{calcite}$ is reported since calcite is dominant and aragonite is insignificant in the sedimentary $CaCO_3$. The $CaCO_3$ saturation state, calculated with CO2SYS from our TA/DIC and $Ca^{2+}$ data, is presented on figure

10

9 for the three domaines. At all stations, the calcite saturation state in pore waters drops in the oxic layer. In the proximal domain (Fig. 9), the saturation state increases immediately below this first drop to reach very high values of around 5 to 10. In the prodelta domain, the saturation state remains very close to 1 at a depth between 5 and 10 cm before increasing to super saturation (3 to 4) below 10 to 15 cm depth. In the distal domain, the saturation state shows no variation below the first drop into the sediment.

## 4 Discussion

### 4.1 Principal diagenetic reactions and their influence on the carbonate system

As the diagenetic transport-reaction network is complex, so are the interactions of these reactions with carbonate chemistry (Krumins et al., 2013). Table 2 summarizes the main diagenetic reactions (simplified) and their impact on DIC and TA pore water concentrations. DIC is always produced by OM mineralization and decreases pH, whereas the TA budget of these reactions and the resulting pH variation can be positive or negative (Soetaert et al., 2007). The dissolution and dissociation of metabolic (or atmospheric) $CO_2$ in seawater results in the formation of carbonic acid (R1), the consumption of $CO_3^{2-}$ and ultimately leads to carbonate dissolution (R2a) (Soetaert et al., 2007; Emerson and Hedges, 2008). Aerobic mineralization consumes $O_2$ and produces $CO_2$, decreasing pH without TA production (R3) and finally decreases $\Omega$. In the sediments, oxygen is also used to reoxidise reduced species, a process that decreases pH even more strongly than aerobic respiration (R4-6) and thus reoxidation decreases $\Omega$ as well (Jourabchi et al., 2005; Glud, 2008). In contrast, anaerobic mineralization causes much weaker pH reductions compared to the oxic processes and can even increase pH (R7-10) (Jourabchi et al., 2005; Soetaert et al., 2007). OM mineralization by nitrate reduction produces DIC and TA, has been related to TA release from the sediments and is even estimated to be a major TA source to the oceans (Thomas et al., 2009). Sulfate reduction is usually associated with a weak decrease in pH, although with significant DIC and TA production (Mucci et al., 2000; Jourabchi et al., 2005). The resulting sulfide ions can either diffuse towards the surface to be oxidized within the oxic layer or precipitate with iron. The precipitation of sulfur minerals does not affect the amount of pore water DIC, but can have major influence on pH and TA (R11-13) (Soetaert et al., 2007). The two reactions R14 and R15 deal with the coupling of sulfate reduction and methanogenesis and its impact on DIC.

In the Rhône River delta sediments, OM mineralization leads to DIC production, and under anoxic conditions, also to TA production. Our results demonstrate strong DIC and TA pore water gradients in the anoxic layer of the sediments indicating high anaerobic respiration rates. As a result, DIC and TA diffuse towards the SWI. No reaction in the oxic zone consumes DIC except potential carbonate precipitation. Our results indicate that more DIC is produced in the sediments than consumed by

11

precipitation of $CaCO_3$. This means, that OM mineralization in the sediments leads to strong DIC fluxes from the sediments into the water column. For TA, the situation is more complicated, as oxidation of reduced species can consume as much TA as has been produced to reduce these species (Table 2). In a 1D system, where no precipitation occurs and no reduced species can be exported, an important fraction of the anaerobic TA would be consumed in the oxic layer. Denitrification forms an exception to this, as the reduced end product $N_2$ of this reaction can escape the sediments. Thus the TA produced by denitrification is not consumed in the oxic sediment layer.

Krumins et al., (2013) reported that the effective TA flux from the sediments into the water column is far less important than the anaerobic TA production due to the TA loss in the oxic layer. Unfortunately, the resolution of the DIC and TA pore water profiles in this current study does not give precise information about the gradients in the oxic layer. Thus, we can only speculate about the oxic TA consumption in this region and related TA fluxes across the SWI. According to Pastor et al. (2011a), 97 % of the reduced species precipitate in the anoxic sediments in the Rhône prodelta. Therefore, the majority of the produced TA is likely released into the water column which can counterbalance the effects of the DIC fluxes and increase the $CO_2$ buffer capacity of the overlaying waters.

## 4.2 The impact of oxic and suboxic processes on the carbonate system

The upper part of the sediment, is defined as the oxic zone, supporting aerobic respiration (R3 – Table 2). Generally, the oxygen penetration depth (OPD) is related to respiration rates (Cai and Sayles, 1996). Aerobic respiration consumes $O_2$ to mineralize organic matter, produces metabolic $CO_2$ in the sediment pore water, increases the DIC concentration, lowers pH and possibly decreases the $CaCO_3$ saturation state (Cai et al., 1993, 1995). The OPD and oxygen fluxes are therefore key parameters to assess the effect of aerobic respiration on calcium carbonate in the sediment (Jahnke et al., 1997; Jahnke and Jahnke, 2004).

In the Rhône River delta, the OPD increases with water depth and distance from the Rhône River mouth as reported in previous studies (Lansard et al., 2008, 2009; Cathalot et al., 2010). These low values of $O_2$ penetration depths are classical for river-dominated ocean margins and they depend mainly on the sedimentation rate, the OM flux, the age and the oxidation state of OM (Lansard et al., 2009, Cathalot et al. 2013). Few *in situ* $O_2$ profiles show oxygen peaks at depth below the OPD. These are likely the effect of sediment bioturbation by the benthic macrofauna. As reported by Bonifácio et al. (2014), the macrofauna community is dominated by polychaetes and the highest activity is found in the prodelta domain. Nevertheless, comparisons between TOU and DOU rates have demonstrated that DOU account for about 80 % of total oxygen uptake rate into the sediments (Lansard et al., 2008). As a consequence, diffusive transport is dominant compared to advective transport and bioturbation (i.e. bioirrigation and bioventilation). Diffusive $O_2$ fluxes calculated from *in situ* 1D micro profiles (Fig. 2) are therefore

12

representative for total oxygen uptake rates. As shown in Fig. 3, the diffusive oxygen fluxes into the sediment decrease exponentially with the distance from the river mouth, from $12.3 \pm 1.1$ mmol $O_2$ m$^{-2}$ d$^{-1}$, close to the Rhône River mouth, to $3.8 \pm 0.9$ mmol $O_2$ m$^{-2}$ d$^{-1}$ offshore. According to Pastor et al., (2011a), the POC flux in the proximal domain is one order of magnitude higher than in the offshore regions of the Rhône prodelta. This OM flux, especially its labile fraction, supports oxygen consumption and is completely mineralized in the oxic layer (Pastor et al., 2011a).

During aerobic respiration, the ratio of oxygen to DIC during OM mineralization is close to 1, according to the stoichiometry of reaction R3 (Table 2). As a result, DIC concentrations increase just below the SWI at all stations (Fig. 5). The balance between $O_2$ flux and carbon oxidation in the sediment is affected by $O_2$-consumption linked to the oxidation of inorganic species produced via anoxic OC degradation ($NH_4^+$, $Fe^{2+}$, $Mn^{2+}$ and $HS^-$). The oxidation of reduced diagenetic products has a profound effect on pore water $O_2$ and pH profiles in $O_2$ limited sediments (Cai and Reimers, 1993). These reactions (R4 to R6), in addition to aerobic bacterial respiration, consume TA and decrease pore water pH and therefore decrease the calcium carbonate saturation state as well.

There is a large contribution of anoxic processes to total OM mineralization in sediments near the Rhône River mouth, certainly due to large inputs of fresh organic material combined with high sedimentation rates (Pastor et al., 2011a). The diagenetic by-products originally produced during anoxic mineralization are almost entirely precipitated and buried in the sediment, which leads to a relatively low contribution of the re-oxidation of reduced products to total oxygen consumption. Still, between 10 to 40 % of the oxygen flux is used to oxidize reduced species of iron and manganese, contributing to lower pH (Pastor et al., 2011a). Again, the upward flux of reduced species in the sediments is higher in the proximal domain than in the others. Offshore, less OM is available and the diagenetic activity is weaker, providing less reduced species from deeper sediment layers. The pH drops below the SWI, caused by all oxic processes, are visible on the *in situ* pH micro profiles and decreases until the OPD is reached (Figs. 2 and 4). As the OPD are smaller and the oxygen fluxes are higher in the proximal domain, the pH minimums are reached at shallower depth in the sediment than in the other domains. The pH drop is lowering $\Omega$ by consuming carbonate ions (Emerson and Hedges, 2008; Jourabchi et al., 2005). The decrease of $\Omega$, due to both aerobic respiration and the oxidation of reduced species, is clearly visible between the first two points located above and below the SWI interface (Fig. 9).

In agreement with current understanding of anoxic diagenesis, the observed pH increase of 0.1 to 0.2 units below the OPD can be attributed to OM mineralization via reduction of iron and manganese (R8 and R9 – Table 2). These anoxic reactions release TA and increase pH in the oxic-anoxic transition zone (Aguilera et al., 2005; Jourabchi et al., 2005). This pH increase and the release of TA create a strong increase in the pore water saturation state ($\Omega$). Previous researches indicated that the turnover of Fe and Mn is high in the sediments close to the river mouth (Pastor et al., 2011a). The first pore water data

13

point sampled in the sediments represents a mixture of oxic and anoxic pore water. Therefore, we potentially over estimate $\Omega$ in the oxic layer based on calculations from pore water concentrations (Cai et al., 2010). Different measurements in the deep sea revealed that $\Omega$ shows a minimum in the oxic layer (Cai et al., 1993, 1995, 1996; Hales and Emerson, 1997). As pH decreased at all stations to the same value, but the TA and DIC gradients at the interface are the strongest in the proximal domain, $\Omega$ should show the highest values in the oxic sediments of the proximal domain and decrease in offshore direction. High TA concentrations in the oxic layer resulting from anoxic OM mineralization below, prevent the carbonate saturation state from getting below 1. Thus, potential dissolution in the oxic layer would most likely occur in the distal domain, but could be inhibited in the proximal domain.

 In contrast to other nearshore environments, nitrate reduction has been shown to account only for 2-5 % of OM mineralization in the sediments of the prodelta of the Rhône whereas other anaerobic mineralization processes account for 30-40 % in the distal domain and up to 90 % in the proximal domain (Pastor et al., 2011a). Nitrate reduction produces less TA than DIC (TA/DIC ratio = 0.8/1) and thus lowers $\Omega$ in the pore waters. Nevertheless denitrification is a net TA source from the sediments to the bottom water as the end product $N_2$ undergoes no further oxidation.

Finding this clear succession of reactions is interesting, particularly the pH profiles that look classical in the aerobic sediment layers sampled from this complex and dynamics system. As OPDs measure only a couple of mm, molecular diffusion is by far the dominant transport process (Peclet number $\gg$ 1 on a scale of the OPD). The microstructure of these sediments is restored very fast after disturbances like resuspension events (Toussaint et al., 2014). Furthermore, the comparison with previous studies shows, that despite the high sediment dynamics in this region, the general biogeochemical tendencies are maintained throughout time.

## 4.3 Sulfate reduction and its impact on carbonate chemistry

With sulfate concentration in seawater around 30 mmol $L^{-1}$, $SO_4^{2-}$ reduction can generate large amounts of DIC and TA during organic matter mineralization through sulfate reduction. Indeed, in organic rich sediments, sulfate reduction can account for the majority of OM mineralization (Gaillard et al., 1989; Jourabchi et al., 2005; Burdige, 2011; Fenschel et al., 2012). Following reaction R9, two units of DIC and TA are produced for one unit of sulfate consumed (Mucci et al., 2000; Krumins et al., 2013).

To estimate the actual $\Delta DIC/\Delta SO_4^{2-}$ ratio due to diagenetic processes, the slope of the correlation between produced DIC ($\Delta DIC$) and consumed sulfates ($\Delta SO_4^{2-}$) in the pore waters (Fig 10) has to be corrected for molecular diffusion following the equation proposed by Berner (1980). Accordingly, we used the diffusion coefficients determined by Li and Gregory (1973). Below 10 cm depth, the observed diffusion corrected $\Delta DIC/\Delta SO_4^{2-}$ ratio equals 1.8 ± 0.02. The deviation of this measured value, from the

14

465  theoretical value of 2 can be linked to higher oxidation states of organic matter which increases the $SO_4^{2-}$ requirement for DIC production (in an extreme case, if methane undergoes oxidation, the $\Delta DIC/\Delta SO_4^{2-}$ ratio equals 1), carbonate precipitation lowering DIC concentrations or methanogenesis that increases DIC without consuming $SO_4^{2-}$ (Burdige and Komada, 2011; Antler et al., 2014). All three factors may interact in the proximal zone. A large OM fraction in this zone is of terrestrial origin, aged

470  and partly oxidized before being deposited (Cathalot et al., 2013). Calcium carbonates precipitate in the pore waters of these sediments (Fig. 7) and lower DIC concentrations. In addition, the presence of methane has been reported by Garcia-Garcia et al., (2006).

As demonstrated by Burdige (2011) and Burdige and Komada (2011), the interaction of all diagenetic pathways are hard to disentangle and do not provide clear evidence of changes in the $\Delta DIC/\Delta SO_4^{2-}$

475  ratio. Nonetheless, the value of the observed $\Delta DIC/\Delta SO_4^{2-}$ ratio (1.8 ± 0.1 ) points towards the dominance of sulfate reduction in the deeper layers of the sediment (below 10 cm depth). Despite all these diverse reactions that affect the $\Delta DIC/\Delta SO_4^{2-}$ ratio, they are balanced in a way that $\Delta DIC$ and $\Delta SO_4^{2-}$ correlate well and do not show a deviation in the slope throughout the whole sediment depth investigated (Figure 10).

480  Sulfate reduction is also attested by the co-production of alkalinity and DIC (Fig. 5) which is by far the most important alkalinity producer in marine sediments (Krumins et al., 2013). Sulfate reduction creates a TA/DIC ratio very close to 1 in the pore waters. This situation is very similar to Mangrove Lake sediments (Mackenzie et al., 1995) where depletion of sulphate is almost complete and DIC and TA concentrations build up to 40 mmol $L^{-1}$ in the sediment pore waters, or to other coastal environments

485  (Burdige, 2011; Antler et al., 2014). No other reaction in the anoxic zone has a TA/DIC production ratio near 1. As pH is buffered, probably by precipitation of FeS and $FeS_2$ (R12), this large increase of alkalinity is accompanied, in the proximal zone, by a large increase of the saturation state of pore waters with respect to calcite (Fig. 9) up to values of oversaturation ($\Omega$) from 5 to 10.

The effect of sulphate reduction and the carbonate saturation state has been a matter of debate since the

490  early work of Ben-Yaakov (1973). Indeed, sulphate reduction produces large quantities of both alkalinity, which increases $\Omega$, and protons, which decrease $\Omega$. This has been summarized in Jourabchi et al.'s model (2005) by estimating that sulphate reduction would lead to decrease of $\Omega$ if it was the only ongoing reaction. The sediments from the proximal area of the Rhône River delta show, on the contrary, that pH stabilizes between 7.2 and 7.6. In these sediments, mineralization is driven by sulphate

495  reduction that generates an increase of saturation state with respect to calcite (Fig. 9). This situation is very similar to Mackenzie et al. (1995) and Mucci et al. (2000) who also showed an increase of $\Omega$ when sulphate reduction is significant. Using a closed system model, Ben Yaakov (1973) estimated that

15

oxidation of HS⁻ coupled to iron hydroxide reduction with FeS precipitation (as in R11 or R12) would buffer or even increase pH.

500 The Rhône River is known to be the most important riverine input of iron into the Mediterranean Sea (Guieu et al., 1991) with an iron content varying between 2 and 4 % in the solid phase discharge. In the proximal zone of the Rhone Delta, dissolved sulphide is absent from the first tens of centimeters in the sediment (Pastor et al., 2011a) indicating that re-oxidation and/or precipitation of sulphide is occurring in these sediments. Pastor et al, (2011a) estimated that sulphides are the limiting factor for pyrite
505 precipitation in this environment. Therefore, Charles et al., (2014) suggested, that OM mineralization in the prodelta of the Rhône could be coupled to pyritisation. With this important FeS coupling, pH is stabilized or tends to increase and a large oversaturation with respect to calcium carbonate is created due to produced carbonate ions.

In the proximal domain, the large super saturation with respect to calcite, induces calcite precipitation as
510 evidenced by a large decrease of dissolved calcium in the pore waters (Gaillard et al., 1989; Boudreau et al., 1992). Indeed, $Ca^{2+}$ concentration decreases by 9 mmol $L^{-1}$ between the bottom water and 25 cm depth in proximal sediments. This precipitation consumes about 10 to 15 % of anaerobically produced DIC and TA. Following R2b, this should affect the TA/DIC ratio, but the observations do not show any deviations of the TA/DIC ratio from 1. The missing TA is likely provided by pyrite formation (R12).

515 In the prodelta domain (Fig. 8), a similar set of reaction involving sulfate reduction and sulphide re-oxidation and precipitation is also visible with lower amplitude as sulfate depletion is only 5 mmol $L^{-1}$. Oversaturation with respect to calcite reaches values ranging from 3-4 only below 15 cm, and the $Ca^{2+}$ decrease is limited and arises deeper. In the distal zone where $\Omega$ is around 2 down to 25 cm, no calcium decrease is visible indicating that precipitation does not occur.

520 As the alkalinity fluxes produced by anaerobic processes are high and likely not much reduced by reoxidation of reduced species in the oxic layer due to iron sulfide precipitation, net TA fluxes of the same order of magnitude than DIC fluxes are likely to occur. Therefore, the alkalinity build up in the anoxic zone could diffuse across the oxic sediment layer and contribute to buffer bottom waters and increase $CO_2$ storage capacity of these waters. The large precipitation of calcium carbonate in the
525 proximal zone may have implications for the $CO_2$ source potential from the sediment. Indeed, calcium carbonate precipitation generates $CO_2$ (R2b) which can then be exported to the water column. In addition, calcium carbonate precipitation consumes TA. However, the order of magnitude of the TA consumption by carbonate precipitation in these sediments is below the quantity of TA produced by sulfate reduction. Without this TA flux, the $pCO_2$ of the bottom waters in the prodelta of the Rhône
530 would likely be much higher than observed.

16

# 5 Conclusions

This study demonstrated that the three major domains of the Rhône River prodelta are characterized by different organic and inorganic particulate carbon interactions. Close to the river mouth, where the carbon turnover is highest, the biogeochemical gradients are the strongest, resulting in high chemical fluxes across the SWI. This confirms that the biogeochemistry in the prodelta region is driven by the import and processing of material from the Rhône River.

The oxic reactions produce $CO_2$ and create a pH drop of 0.6 to 0.8 pH units and reduce $\Omega$. As a consequence, calcium carbonate might dissolve in the oxic layer, but the saturation state of bottom waters and pore waters just below the OPD suggest that this is unlikely to happen. The majority of oxygen is used for OM mineralization as most of reduced species precipitate in anoxic sediments and do not contribute to oxygen consumption. The mineralization of OM, presumably by Fe and Mn oxides, increases pH and $\Omega$ below the oxic layer to several mm in depth.

The strong TA and DIC gradients observed in the sediments of the Rhône River prodelta suggest that OM mineralization is dominated by anaerobic processes. Close to the river mouth, where the OC content in the sediments is highest, sulfate reduction is the dominant mineralization process for OM degradation creating a strong coupling between TA and DIC in pore water profiles. Despite its theoretical lowering effect on pH, sulfate reduction is related to an increase of $\Omega$ by important alkalinity production and via the simultaneous pH increase by precipitation of iron-sulfate-minerals. As a result, pore waters are over saturated at all sampled stations. Calcium carbonate precipitation occurs in the proximal and in the prodelta domain, depleting the majority of dissolved calcium ions in the proximal domain. This carbonate precipitation could represent an additional $CO_2$ source from the sediments to the water column, but is outbalanced by TA production by sulfate reduction. Due to this important anoxic TA production, the $pCO_2$ of bottom waters remain relatively low compared to the high release of DIC due to OM mineralization.

17

565

# References

Aguilera, D. R., Jourabchi, P., Spiteri, C. and Regnier, P.: A knowledge-based reactive transport approach for the simulation of biogeochemical dynamics in Earth systems: earth system dynamics, Geochem. Geophys. Geosy., 6, 1-18, 2005.

Aller, R. C.: Mobile deltaic and continental shelf muds as suboxic, fluidized bed reactors, Mar. Chem., 61, 143-155, 1998.

Aller, R. C. and Blair, N. E.: Carbon remineralization in the Amazon-Guianas tropical mobile mudbelt: A sedimentary incinerator, Cont. Shelf. Reas., 26, 2241-2259, 2006.

Andersson, A. J., Mackenzie, F. T., Lerman, A.: Coastal ocean and carbonate system in the high $CO_2$ world of the anthropocene, AM. J. Sci., 305, 875-918, 2005.

Andrews, D. and Bennet, A.: Measurements of diffusivity near the sediment-water interface with a fine-scale resistivity probe, Geochim. et Cosmochim. Acta, 45, 2169-2175, 1981.

Antler, G., Turchyn, A. V., Herut, B. Davies, A. and Rennie, V. C. F.: Sulfur and oxygen isotope tracing of sulfate driven anaerobic methane oxidation in estuarine sediments, Estuar. Coast. Shelf Sci., 142, 4-11, 2014.

Arndt, S., Jørgensen, B. B., LaRowe, D. E., Middelburg, J. J., Pancost, R. D. and Regnier, P.: Quantifiying the degradation of organic matter in marine sediments: A review and synthesis, Earth Sci. Rev., 123, 53-86, 2013.

Bauer, J. E., Cai, W.-J., Raymond, P. A., Bianchi, T. S., Hopkinson, C. S. and Regnier, P. A. G.: The changing carbon cycle of the coastal ocean, Nature, 504 (7478), 61–70, 2013.

Ben-Yaakov, S.: pH buffering of pore water of recent anoxic marine sediments, Limnol. Oceanogr., 18, 86–94, 1973.

Berner, R. A.: Early diagenesis: A theoretical approach, Princeton University Press, 241 pp., 1980.

18

570 Boudreau, B. P., Canfield, D. E. and Mucci, A.: Early diagenesis in a marine sapropel, Mangrove Lake, Bermuda, Limnol. and Oceanogr., 37, 8, 1738-1753, 1992.

Bourgeois, S., Pruski, A. M., Sun, M.-Y., Buscail, R., Lantoine, F., Vétion, G., Rivière, B. and Charles, F.: Distribution and lability of land-derived organic matter in the surface sediments of the Rhône prodelta and the adjacent shelf (Mediterranean sea, France): a multi proxy study, Biogeosciences, 8,
575 3107-3125, 2011.

Broecker, W. S. and Peng, T.-H.: Gas exchange rates between air and sea. Tellus, 26, 21–35, 1974.

Burdige, D. J., Zimmerman, R. C., and Hu, X.: Rates of carbonate dissolution in permeable sediments estimated from pore-water profiles: The role of sea grasses. Limnol. and Oceanogr., 53, 549-565, 2008.

Burdige, D. J., Hu, X. and Zimmermann, R. C.: The widespread occurence of coupled carbonate dissolution / reprecipitation in surface sediments on the Bahamas Bank, AM. J. Sci., 310, 492-521, 2010.

Burdige, D. J.: Estuarine and Coastal Sediments - Coupled Biogeochemical Cycling, Treatise Esturarine Coast. Sci., 5, 279–316, 2011.

Burdige, D. J. and Komada, T.: Anaerobic oxidation of methane and the stoichiometry of remineralization processes in continental margin sediments, Limnol. Oceanogr., 56(5), 1781–1796, 2011.

Cai, W. J., and Reimers, C. E.: The development of pH and $p$CO$_2$, microelectrodes for studying the carbonate chemistry of pore waters near the sediment-water interface, Limnol. and Oceanogr., 38, 1762-1773, 1993.

Cai, W. J., Reimers, C. E., and Shaw, T.: Microelectrode studies of organic carbon degradation and calcite dissolution at a California Continental rise site, Geochim. et Cosmochim. Acta, 59, 497-511, 1995.

Cai, W.-J., and Sayles, F. L.: Oxygen penetration depths and fluxes in marine sediments, Mar. Chem., 52, 123-131, 1996.

Cai, W.-J., Zhao, P. and Wang, Y.: pH and pCO$_2$ microelectrode measurements and the diffusive behaviour of carbon dioxide species in coastal marine sediments, Mar. Chem. 70, 133-148, 2000.

Cai, W.-J., Luther III, G. W., Cornwell, J. C. and Giblin, A. E.: Carbon Cycling and the Coupling Between Proton and Electron Transfer Reactions in Aquatic Sediments in Lake Champlain, Aquat. Geochem, 421-446, 2010.

19

Cai, W.-J.: Estuarine and Coastal Ocean Carbon Paradox: $CO_2$ Sinks or Sites of Terrestrial Carbon Incineration?, Annu. Rev. Mar. Sci., 3, 123–145, 2011.

Cathalot, C., Rabouille, C., Pastor, L., Deflandre, B., Viollier, E., Buscail, R., Grémare, A., Treignier, C. and Pruski, A.: Temporal variability of carbon recycling in coastal sediments influenced by rivers: assessing the impact of flood inputs in the Rhône River prodelta., Biogeosciences, 7, 1187-1205, 2010.

Cathalot, C., Rabouille, C., Tisnérat-Laborde, N., Toussaint, F., Kerhervé, P., Buscail, R., Loftis, K., Sun, M.-Y., Tronczynski, J., Azoury, S., Lansard, B., Treignier, C., Pastor, L. and Tesi, T.: The fate of river organic carbon in coastal areas: A study in the Rhône River delta using multiple isotopic ($\delta$13C, $\Delta$14C) and organic tracers, Geochim. Cosmochim. Acta, 118, 33–55, 2013.

Charles, F., Coston-Guarini, J., Lantoine, F., Guarini, J.-M. and Yücel, M.: Ecogeochemical fate of coarse organic particles in sediments of the Rhône River prodelta, Estuar. Coast. Shelf Sci., 141, 97–103, 2014.

Charmasson, S., Radakovitch, O., Arnaud, M., Bouisset, P. and Pruchon, A.-S.: Long-core profiles of ^{137}Cs, [134]Cs, ^{60}Co and ^{210}Pb in sediment near the Rhône River (Northwestern Mediterranean Sea), Estuaries, 21, 367–378, 1998.

Chen, C.-T. A. and Borges, A. V.: Reconciling opposing views on carbon cycling in the coastal ocean: Continental shelves as sinks and near-shore ecosystemsas sources of atmospheric $CO_2$ Deep-Sea Res. PT II, 56, 578–590, 2009.

Chen, C.-T. A., Huang, T.-H., Fu, Y.-H., Bai, Y. and He, X.: Strong sources of $CO_2$ in upper estuaries become sinks of $CO_2$ in large river plumes, Current Opinion in Environmental Sustainability, 4, 179-185, 2012.

Clayton, T. D. and Byrne, R. H.: Spectrophotometric seawater pH measurements: total hydrogen ion concentration scale calibration of m-cresol purple and at-sea results, Deep Sea Res. Part Oceanogr. Res. Pap., 40, 2115–2129, 1993.

Dai, M., Yin, Z., Meng, F., Liu, Q., Cai, W.-J.: Spatial distribution of riverine DOC inputs to the ocean: an updated global synthesis, Current Opinion in Encvironmental Sustainability, 4, 170-178, 2012.

Dickson, A.G., Sabine, C.L. and Christian, J.R.: Guide to best practices for ocean $CO_2$ measurements. PICES Special Publication 3, 2007.

20

Durrieu de Madron, X., Abassi, A., Heussner, S., Monaco, A., Aloisi, J. C., Radakovitch, O., Giresse, P., Buscail, R. and Kerherve, P.: Particulate matter and organic carbon budgets for the Gulf of Lions (NW Mediterranean), Oceanol. Acta, 23, 717–730, 2000.

Emerson, S. R. and Hedges, J. I.: Chemical Oceanography and the Marine Carbon Cycle, Cambridge University Press, 2008.

Estournel, C., Kondrachoff, V., Marsaleix, P. and Vehil, R.: The plume of the Rhone: numerical simulation and remote sensing, Cont. Shelf. Res., 17, 899-924, 1997.

Fenschel, T., King, G. M. and Blackburn, T. H.: Bacterial Biogeochemistry: The Ecophysiology of Mineral Cycling, 3rd ed., Academic Press (Elsevier)., 2012.

Froelich, P., Klinkhamm, G. P., Bender, M., Luedtke, N. A., Heath, G. R., Cullen, D., Dauphin, P., Hammond, D., Hartman, B. and Maynard, V.: Early oxidation of organic matter in pelagic sediments of the eastern equatorial Atlantic: suboxic diagenesis, Geochim. Cosmochim. Acta, 43, 1075–1090, 1979.

Gaillard, J.-F., Pauwels, H. and Michard, G.: Chemical diagenesis in coastal marine sediments, Oceanol. Acta, 12, 175-187, 1989.

García-García, A., Orange, D., Lorenson, T., Radakovitch, O., Tesi, T., Miserocchi, S., Berné, S., Friend, P. L., Nittrouer, C. and Normand, A.: Shallow gas off the Rhône prodelta, Gulf of Lions, Mar. Geol., 234, 215–231, 2006.

Glud, R. N.: Oxygen dynamics of marine sediments, Mar. Biol. Res., 4, 243-289

Got, H. and Aloisi, J. C.: The Holocene sedimentation on the Gulf of Lions margin: a quantitative approach, Cont. Shelf. Res., 10, 841-855, 1990.

Grasshoff, K. Ehrhardt, M, and K. Kremling.: Methods of Seawater Analysis. Grasshoff, Ehrhardt and Kremling, eds. Verlag Chemie GmbH. 419 pp., 1983.

Guieu, C., Martin, J. M., Thomas, A. J. and Elbaz-Poulichet, F.: Atmospheric Versus River Inputs of Metals to the Gulf of Lions, Total Concentrations, Partitioning and Fluxes, Mar. Poll. Bulletin, 22, 176-183, 1991.

Hales, B. and Emerson, S.: Calcite dissolution in sediments of the Cera Rise: In situ measurements of porewater $O_2$, pH and $CO_{2(aq)}$, Geochim. et Cosmochim. Acta, 61, 501-514, 1997.

Hedges, J. I. and Keil, R. G.: Sedimentary organic matter preservation: an assessment and speculative synthesis, Mar. Chem., 49, 81-115, 1995.

580

21

Jahnke, R. A., Craven, D. B., McCorkle, D. C., and Reimers, C. E.: CaCO$_3$ dissolution in California continental margin sediments: the influence of organic matter remineralization, Geochim. et Cosmochim. Acta, 61, 3587-3604, 1997.

Jahnke, R. A., and Jahnke, D. B.: Calcium carbonate dissolution in deep sea sediments: reconciling microelectrode, pore water and benthic flux chamber results, Geochim. et Cosmochim. Acta, 68, 47-59, 2004.

Jourabchi, P., Van Cappellen, P. and Regnier, P.: Quantitative interpretation of pH distributions in aquatic sediments: A reaction-transport modeling approach, Am. J. Sci., 305, 919–956, 2005.

Krumins, V., Gehlen, M., Arndt, S., Van Cappellen, P. and Regnier, P.: Dissolved inorganic carbon and alkalinity fluxes from coastal marine sediments: model estimates for different shelf environments and sensitivity to global change, Biogeosciences, 10, 371–398, 2013.

Lansard, B., Rabouille, C., Denis, L. and Grenz, C.: In situ oxygen uptake rates by coastal sediments under the influence of the Rhône River (NW Mediterranean Sea), Cont. Shelf Res., 28, 1501–1510, 2008.

Lansard, B., Rabouille, C., Denis, L. and Grenz, C.: Benthic remineralization at the land–ocean interface: A case study of the Rhône River (NW Mediterranean Sea), Estuar. Coast. Shelf Sci., 81, 544–554, 2009.

Laruelle, G. G., Dürr, H. H., Lauerwald, R., Hartmann, J., Slomp, C. P., Goossens, N. and Regnier, P. A. G.: Global multi-scale segmentation of continental and coastal waters from the watersheds to the continental margins, Hydrol. Earth Syst. Sci, 17, 2029-2051, 2013.

Lewis, E. and Wallace, D. W. R, Program developed for CO$_2$ system calculations. ORNL/CDIAC-105, Carbon Dioxide Information Analysis Center, US Department of Energy, Oak Ridge National Laboratory, Tennessee: http://cdiac.esd.ornl.gov/oceans/co2rprt.html, 1998.

Li, Y.-H. and S. Gregory: Diffusion of ions in sea water and in deep-sea sediments, Geochim. et Cosmochim. Acta, 88, 703-714, 1974.

Lueker, T. J., Dickson, A. G., Keeling, C. D.: Ocean pCO$_2$ calculated from dissolved inorganic carbon, alkalinity, and equations for K$_1$ and K$_2$ : validation based on laboratory measurements of CO$_2$ in gas and seawater at equilibrium, Mar. Chem., 70, 105-119, 2000.

585

590

Mackenzie, F. T. Vink, S., Wollast, R. and Chou, L.: Comparative Geochemistry of Marine Saline Lakes, Physics and Chemistry of Lakes, 2nd edition, Springer-Verlag, Berlin, 265-278, 1995

McKee, B.A., Aller, R.C., Allison, M.A., Bianchi, T.S. and Kineke, G.C.: Transport and transformation of dissolved and particulate materials on continental margins influenced by major rivers: benthic boundary layer and seabed processes, Cont. Shelf. Res.,24, 899-926, 2004.

Millero, F. J.: Thermodynamics of the carbon dioxide system in seawater, Geochim. Cosmochim. Acta, 43, 1651–1661, 1979.

Millero, F. J.: Thermodynamics of the carbon dioxide system in the oceans, Geochim. et Cosmochim. Acta, 59, 661-677, 1995.

Mojtahid, M., Jorissen, F., Lansard, B. and Fontanier, C.: Microhabitat selection of benthic foraminifera in sediments off the Rhône River mouth (NW Mediterranean), J. Foramin. Res., 40(3), 231–246, 2010.

Mucci, A.: The solubility of calcite and aragonite in seawater at various salinities, temperatures and one atmosphere total pressure, AM. J. Sci., 283, 780-799, 1983.

Mucci, A., Sundby, B., Gehlen, M., Arakaki, T., Zhong, S. and Silverberg, N.: The fate of carbon in continental shelf sediments of eastern Canada: a case study, Deep Sea Res. Part II Top. Stud. Oceanogr., 47, 733–760, 2000.

Nouet, J. and Bassinot, F.: Dissolution effects on the crystallography and Mg/Ca content of planktonic foraminifera *Gloorotalia tumida* (Rotaliina) revealed by X-ray diffractometry, Geochem. Geophy. Geosy., 8, Q10007, doi:10.1029, 2007.

Orr, J. C., Epitalon, J.-M. and Gattuso, J.-P.: Comparison of ten packages that compute ocean carbonate chemistry, Biogeosciences, 12, 1483–1510, 2015.

Pastor, L., Cathalot, C., Deflandre, B., Viollier, E., Soetaert, K., Meysmann, F.J.R., Ulses, C., Metzger, E. and Rabouille, C.: Modeling biogeochemical processes in sediments from the Rhône River prodelta area (NW Mediterranean Sea), Biogeosciences, 8, 1351-1366, 2011a.

Pastor, L., Deflandre, B., Viollier, E., Cathalot, C., Metzger, E., Rabouille, C., Escoubeyrou, K., Lloret, E., Pruski, A. M. and Vétion, G.: Influence of the organic matter composition on benthic oxygen demand in the Rhône River prodelta (NW Mediterranean Sea), Cont. Shelf Res., 31, 1008-1019, 2011b.

Pont D.: Les débits solides du Rhône à proximité de son embouchure : données récentes (1994-1995) / The discharge of suspended sediments near to the mouth of the Rhône recent statistics (1994-1995), Revue de géographie de Lyon, 72, 23-33, 1997.

Rabouille, C., Denis, L., Dedieu, K., Stora, G., Lansard, B. and Grenz, C.: Oxygen demand in coastal marine sediments: comparing in situ microelectrodes and laboratory core incubations, J. Exp. Mar. Biol. Ecol., 285, 49–69, 2003.

Revsbech, N. P.: An oxygen microsensor with a guard cathode, Limnol. and Oceanogr., 34, 474-478, 1989.

Roussiez, V., Aloisi, J.-C., Monaco, A. and Ludwig, W.: Early muddy deposits along the Gulf of Lions shoreline: A key for a better understanding of land-to-sea transfer of sediments and associated pollutant fluxes, Mar. Geol., 222-223, 345–358, 2005.

Roussiez, V., Ludwig, W., Monaco, A., Probst, J.-L., Bouloubassi, I., Buscail, R. and Saragoni, G.: Sources and sinks of sediment-bound contaminants in the Gulf of Lions (NW Mediterranean Sea): A multi-tracer approach, Cont. Shelf Reas. 26, 1843-1857, 2006.

Sempéré, R., Charrière, B., Van Wambeke, F. and Cauwet, G.: Carbon inputs of the Rhone River to the Mediterranean Sea: Biogeochemical implications, Glob. Biogeochem. Cycles, 14, 669-681, 2000.

Soetaert, K., Hofmann, A. F., Middelburg, J. J., Meysman, F. J. R. and Greenwood, J.: The effect of biogeochemical processes on pH, Mar. Chem., 105, 30-51, 2007.

Tabatai, M. A.: A rapid method for determination of sulfate in water samples, Environ. Lett., 7, 237–243, 1974.

Thomas, H., Schiettecatte, L.-S., Suykens, K., Koné, Y. J. M., Shadwick, E. H., Prowe, A. E. F., Bozec, Y., de Baar, H. J. W. and Borges, A. V.: Enhanced ocean carbon storage from anaerobic alkalinity generation in coastal sediments, Biogeosciences, 6, 267-274, 2009.

Toussaint F., Rabouille, C., Cathalot, C., Bombled, B., Abchiche, A., Aouji, O., Buchholtz, G., Clemençon, A., Geyskens, N., Répécaud, M., Pairaud, I., Verney, R. and Tisnérat-Laborde, N.: A new device to follow temporal variations of oxygen demand in deltaic sediments: the LSCE benthic station, Limnol. Oceanogr.: Methods, 12, 729-741, 2014

Van Cappellen, P. and Wang, Y.: Cycling of iron and Manganese in surface sediments: A general theory for the coupled transport and reaction of carbon, oxygen, nitrogen, sulfur, iron and manganese, AM J Sci., 296, 197-243, 1996.

**Figure captions**

595

Figure 1: Map of the Rhône River mouth (Northwestern Mediterranean Sea) with the stations investigated during the DICASE cruise in June 2014. The ocean bathymetry (in m) is indicated by the continuous lines.

600 Figure 2: All *in situ* oxygen micro profiles measured during the DICASE cruise, in the proximal, prodelta and distal domains. The sediment-water interface is marked by a horizontal line (depth = 0).

Figure 3: Diffusive oxygen uptake (DOU) across the sediment-water interface in function of the distance from the Rhône River mouth. The fluxes decrease exponentially following $DOU = F_{min} + Ae^{(-x/t)}$
605 with $F_{min}$ being the flux in the offshore region, x the distance to the river mouth in km and, A and t being the numerical constants. Error bars are standard deviations between the diffusive fluxes calculated from the 5 single oxygen profiles measured at each station.

Figure 4: All $pH_t$ micro profiles measured during the DICASE cruise in the proximal, prodelta and
610 distal domains. The sediment-water interface is marked by a horizontal line.

Figure 5: DIC (black) and TA (red) pore water profiles in the first 40 cm of sediment in the proximal, the prodelta and the distal domains. For a better visibility of the profiles in each domain, the scale of the concentrations has been individually adjusted for each domain.

615

Figure 6: Calculated $pH_t$ pore water profiles of the proximal, the prodelta and the distal domains. The error bars are estimations of the error propagation from the measured data in the calculation.

Figure 7: Pore water concentrations of $Ca^{2+}$ (mmol $L^{-1}$); proximal domain in red, prodelta domain in blue
620 and distal domain in black. The error bars represent the uncertainties of the ICP-AES measurements.

25

Figure 8 : Sulfate profiles measured in the pore waters (mmol L$^{-1}$) of the proximal, the prodelta and in the distal domains

625　Figure 9: Pore water calcium carbonate saturation state ($\Omega$) of the proximal, prodelta and distal domain. The saturation limit for calcium carbonates dissolution/precipitation ($\Omega$ =1) is marked by a vertical line.

Figure 10: Scatter plot of $\Delta$DIC vs $\Delta$SO$_4^{2-}$ with linear regression. $\Delta$ designates the difference between the corresponding pore water and bottom water concentration. The slope of the correlation is -1.65 +/-
630　0.017 with a correlation coefficient of r$^2$ = 0.992.

**Figures**

635

640



Figure 1

**Proximal Domain**      **Prodelta Domain**      **Distal Domain**

Figure 2

$$DOU = 3.49 + 18.47 \exp(-dist/2.05)$$
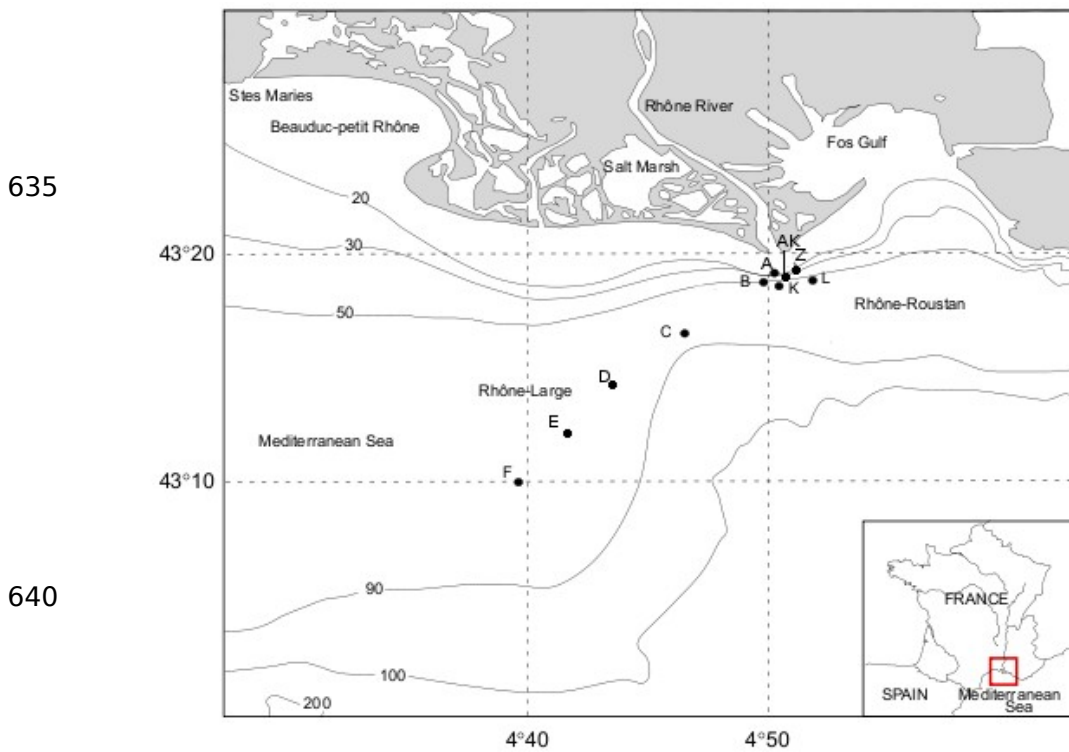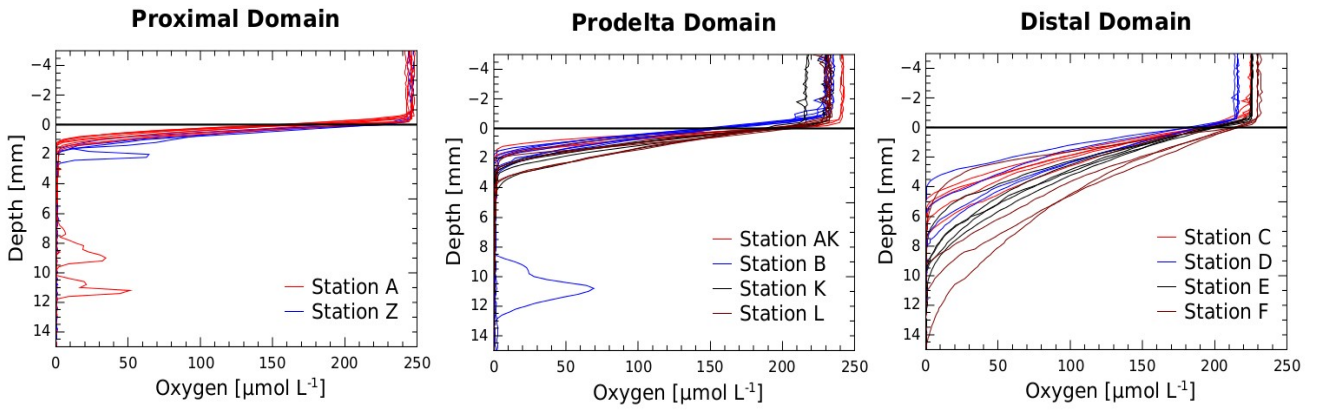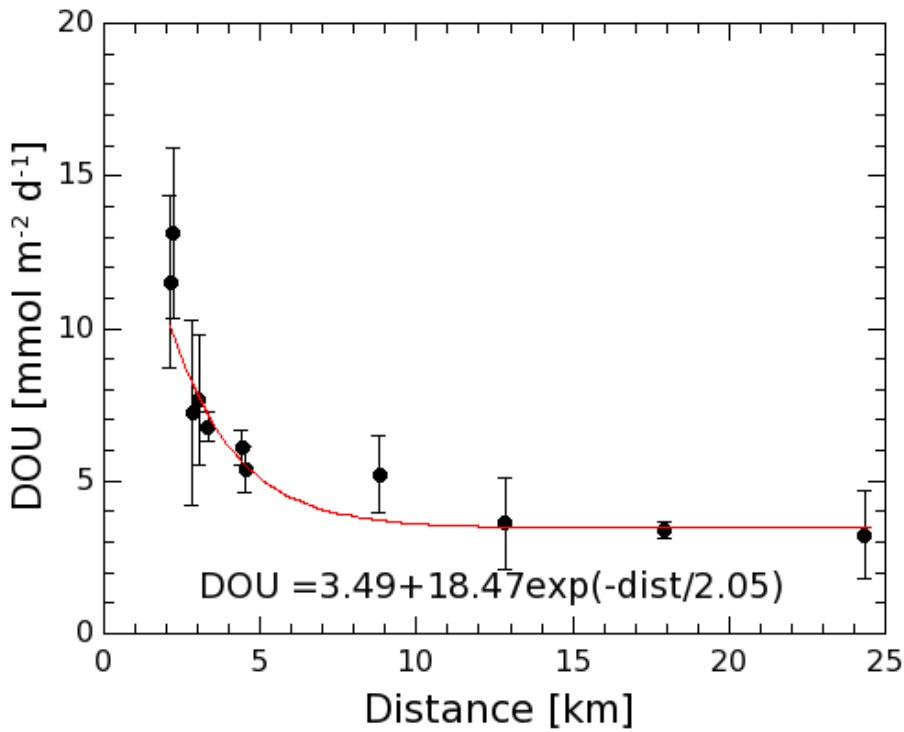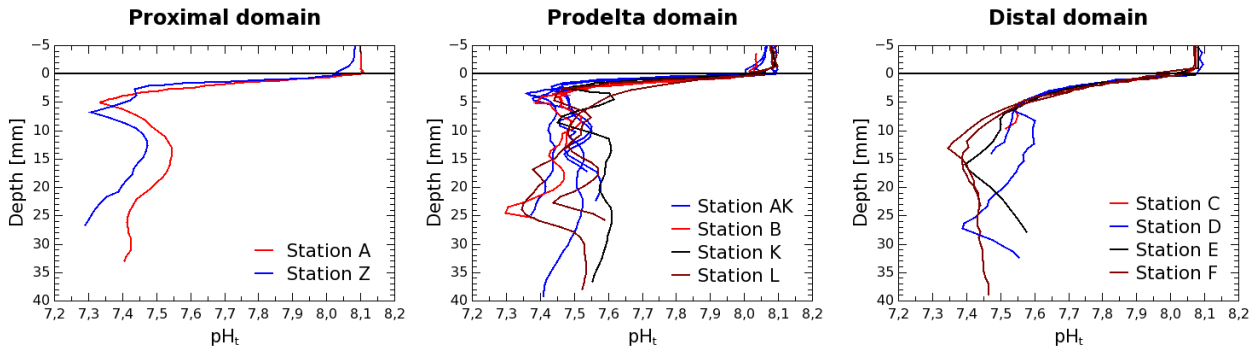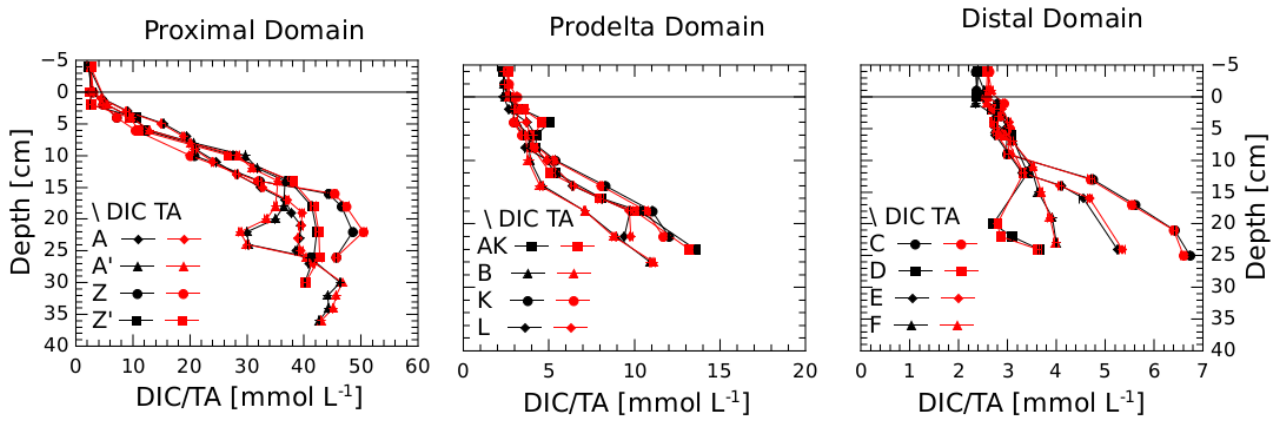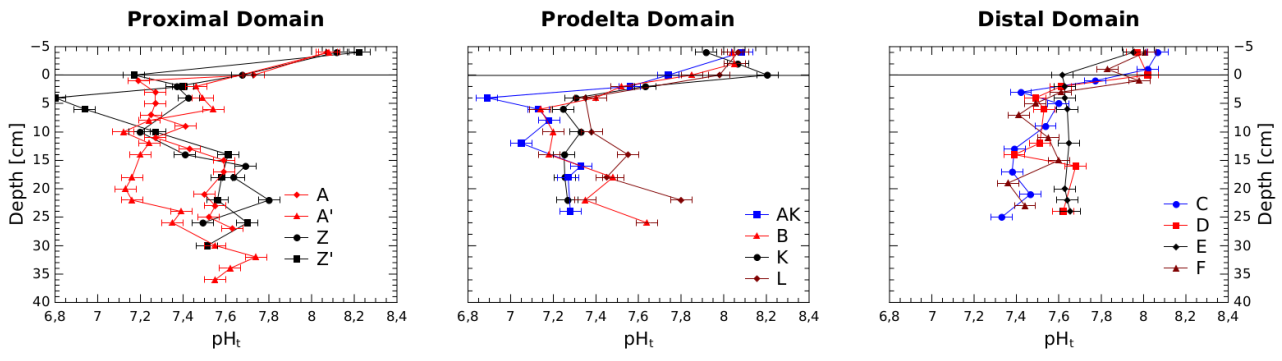
Figure 3

Figure 4
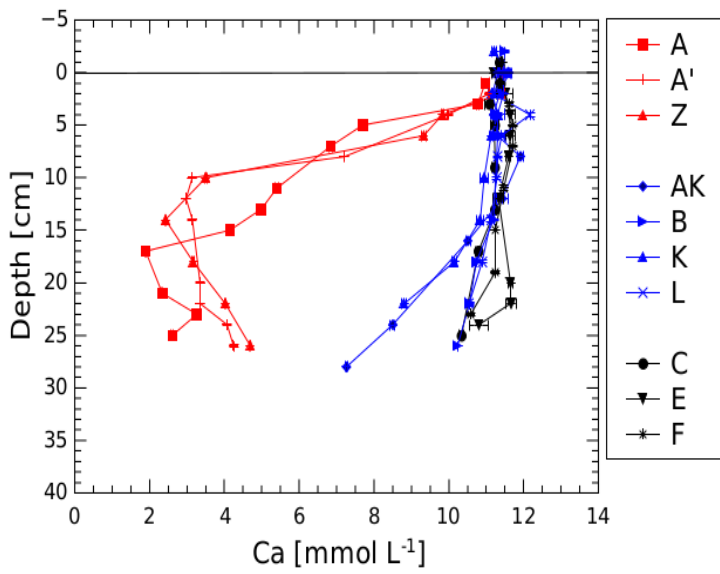
Figure 5
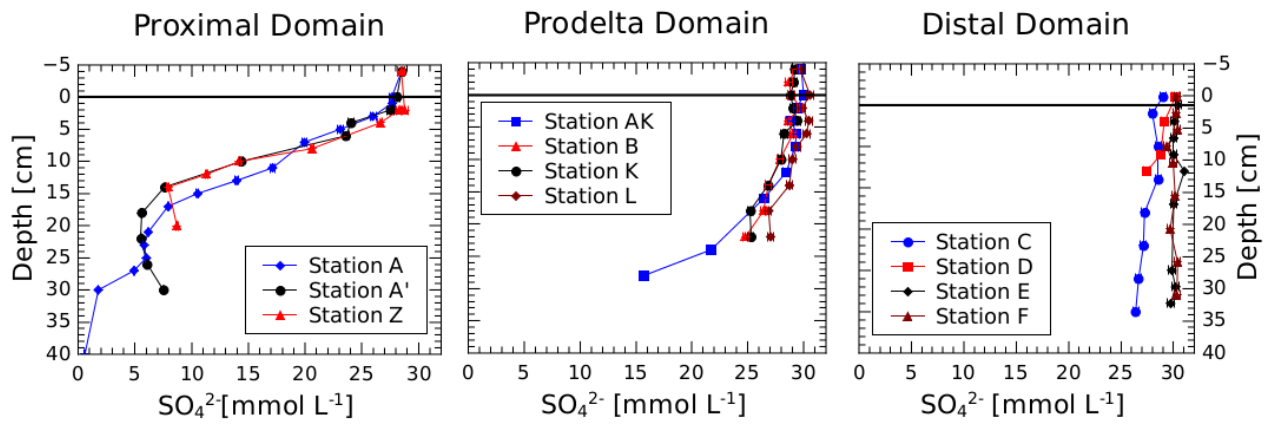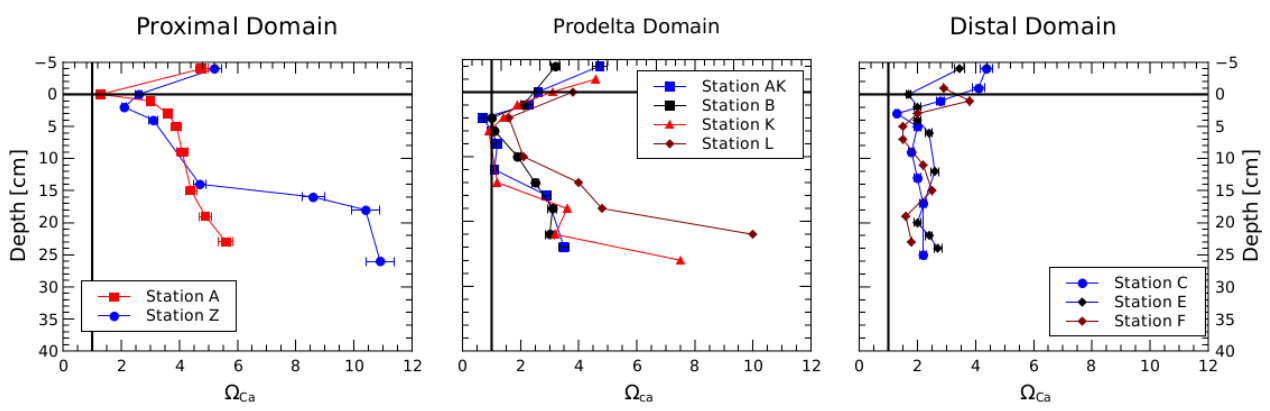
Figure 6

Figure 7

Figure 8
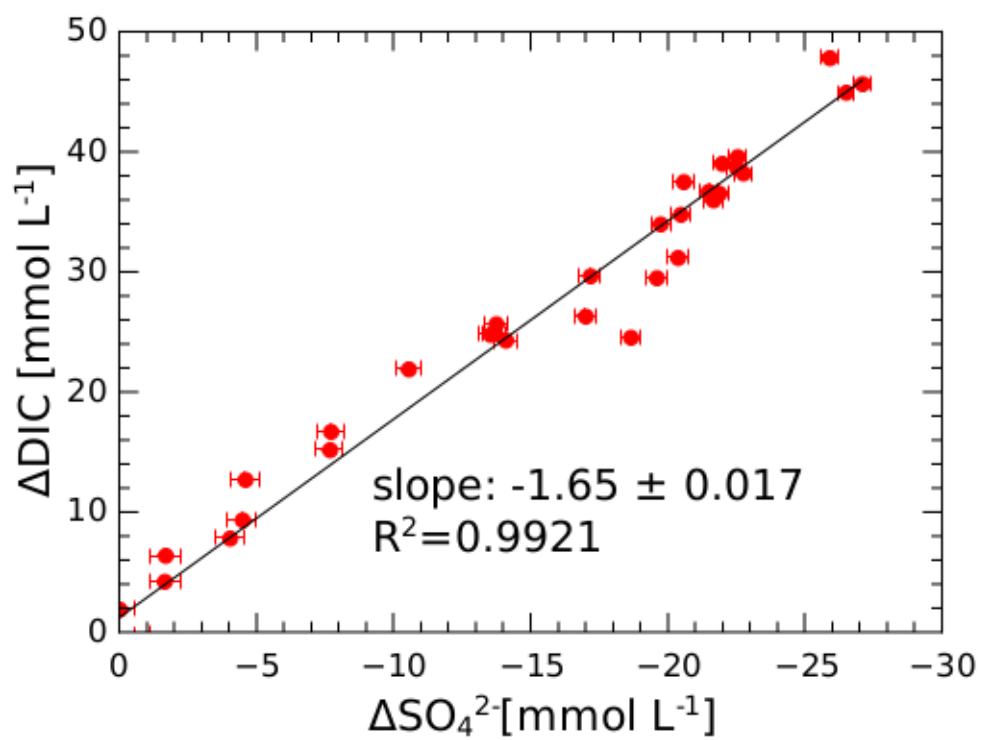


695    Figure 9

700

Figure 10

**Tables**

Table 1: Stations investigated during the DICASE cruise in June 2014 with the main properties of bottom waters; dist = distance from the Rhône river mouth

| Station | Long. (°E) | Lat. (°N) | Dist. [km] | Depth [m] | T [°C] | Salinity | $O_2$ [µmol L$^{-1}$] | DIC [µmol L$^{-1}$] | TA [µmol L$^{-1}$] | $pH_t$ | $SO_4^{2-}$ [mmol L$^{-1}$] | $pCO_2$ (calculated) [µatm] |
|---|---|---|---|---|---|---|---|---|---|---|---|---|
| Z, Z' | 4.865 | 43.317 | 2.2 | 18.0 | 16.0 | 37.5 | 244.0 ± 0.3 | 2330 ± 1 | 2648 ± 3 | 8.118 ± 0.003 | 28.4 ± 0.3 | 364.1 |
| A, A' | 4.851 | 43.312 | 2.1 | 18.3 | 16.8 | 37.7 | 245.1 ± 0.3 | 2323 ± 4 | 2613 ± 17 | 8.072 ± 0.004 | 28.2 ± 0.4 | 407.3 |
| AK | 4.856 | 43.307 | 2.8 | 48.1 | 15.8 | 37.4 | 240.8 ± 0.1 | 2335 ± 4 | 2623 ± 3 | 8.085 ± 0.011 | 29.7 ± 0.3 | 393.6 |
| B | 4.818 | 43.295 | 3.0 | 66.2 | 15.0 | 37.7 | 213.2 ± 0.8 | 2372 ± 5 | 2628 ± 2 | 8.039 ± 0.015 | 28.7 ± 0.3 | 446.1 |
| K | 4.856 | 43.302 | 3.3 | 60.5 | 14.9 | 37.7 | 226.4 ± 0.2 | 2351 ± 5 | 2538 ± 5 | 7.916 ± 0.002 | 29.1 ± 0.3 | 596.6 |
| L | 4.885 | 43.304 | 4.4 | 58.2 | 15.2 | 37.6 | 230.9 ± 0.6 | 2340 ± 2 | 2612 ± 5 | 8.066 ± 0.002 | 29.7 ± 0.3 | 412.4 |
| C | 4.773 | 43.271 | 8.8 | 75.0 | 14.4 | 37.7 | 225.6 ± 0.4 | 2354 ± 2 | 2621 ± 10 | 8.067 ± 0.004 | 29.0 ± 0.3 | 411.5 |
| D | 4.738 | 43.256 | 12.8 | 80.0 | 14.9 | 37.6 | 214.5 ± 0.5 | 2388 ± 8 | 2605 ± 3 | 7.970 ± | 30.2 ± 0.3 | 531.3 |

|  |  |  |  |  |  |  |  |  |  | 0.002 |  |  |
|---|---|---|---|---|---|---|---|---|---|---|---|---|
| E | 4.685 | 43.219 | 17.9 | 77.3 | 14.3 | 37.7 | 226.3 ± 0.3 | 2391 ± 6 | 2594 ± 5 | 7.952 ± 0.004 | 30.4 ± 0.3 | 553.3 |
| F | 4.649 | 43.164 | 24.3 | 77.0 | 14.8 | 37.7 | 230.2 ± 0.1 | 2364 ± 4 | 2600 ± 24 | 8.008 ± 0.006 | 30.3 ± 0.3 | 478.4 |

710

Table 2: Diagenetic reactions and their effect on the carbonate system (TA, DIC, pH and $\Omega$)

|  |  | Reaction | ΔTA/ΔDIC | ΔpH | Δ $\Omega$ |
|---|---|---|---|---|---|
|  | **Carbonate chemistry** |  |  |  |  |
| R1 | $CO_2$ dissolution | $CO_2 + H_2O \leftrightarrow H_2CO_3 \leftrightarrow HCO_3^- + H^+ \leftrightarrow CO_3^{2-} + 2H^+$ |  | - | - |
| R2a | Carbonate dissolution | $CaCO_3 + H_2O + CO_2 \rightarrow Ca^{2+} + 2HCO_3^-$ | + 2/1 | + | + |
| R2b | Carbonate precipitation | $Ca^{2+} + 2\,HCO_3^- \rightarrow CaCO_3 + H_2O + CO_2$ | -2/-1 | - | - |
|  | **Aerobic reactions** |  |  |  |  |
| R3 | Aerobic mineralization | $CH_2O + O_2 \rightarrow HCO_3^- + H^+$ | 0/1 | - | - |
| R4 | Nitrification | $NH_4^+ + 2O_2 \rightarrow NO_3^- + H_2O + 2H^+$ | -2/0 | - | - |

| | | | | | |
|---|---|---|---|---|---|
| R5 | Iron oxidation | $4Fe^{2+}+O_2+10H_2O \rightarrow 4Fe(OH)_3+8H^+$ | -8/0 | - | - |
| R6 | Manganese oxidation | $2Mn^{2+} + O_2 + 4HCO_3^- \rightarrow 2MnO_2 + 4CO_2 + 2H_2O$ | -4/0 | - | - |
| | **Anaerobic Reactions** | | | | |
| R7 | Nitrate reduction | $CH_2O+0.8\,NO_3^-+0.8\,H^+ \rightarrow CO_2+0.4\,N_2+1.4\,H_2O$ | 0.8/1 | - | - |
| R8 | Manganese reduction | $CH_2O+2MnO_2+3H^+ \rightarrow HCO_3^-+2Mn^{2+}+2H_2O$ | 4/1 | + | + |
| R9 | Iron reduction | $CH_2O+4Fe(OH)_3+7H^+ \rightarrow HCO_3^-+4Fe^{2+}+10H_2O$ | 8/1 | + | + |
| R10 | Sulfate reduction | $CH_2O+\frac{1}{2}SO_4^{2-} \rightarrow HCO_3^-+\frac{1}{2}HS^-+\frac{1}{2}H^+$ | 1/1 | - | |
| R11 | FeS precipitation | $Fe^{2+}+HS^- \rightarrow FeS+H^+$ | -2/0 | - | - |
| R12 | FeS precipitation with sulfate recycling | $8Fe(OH)_3+9HS^-+7H^+ \rightarrow 8FeS+SO_4^{2-}+20H_2O$ | -2/0 | + | + |
| R14 | Pyrite precipitation | $8Fe(OH)_3+15HS^-+SO_4^{2-}+17H^+ \rightarrow 8FeS_2+28H_2O$ | 2/0 | + | + |
| R15 | Anaerobic methane oxidation | $CH_4+SO_4^{2-} \rightarrow HS^-+HCO_3^-+H_2O$ | 2/1 | + (if pH < 7.9) | + |
| R16 | Methanogenesis | $CH_2O \rightarrow \frac{1}{2}CH_4+\frac{1}{2}CO_2$ | 0/0.5 | - | - |

715